Geologische Rundschau **81/2** | 515–543 | Stuttgart 1992

Contraints on the evolution of the Mid German Crystalline Rise – a study of outcrops west of the river Rhine

By TH. FLÖTTMANN, Adelaide and O. ONCKEN, Potsdam*)

With 16 figures and 2 tables

Zusammenfassung

Eine Reihe kleinerer Aufschlüsse an der westlichen Rheingrabenrandschulter geben einen Einblick in die westliche Fortsetzung der Mitteldeutschen Kristallinschwelle. Mit der Trennung von rhenohercynischer und saxothuringischer Zone markiert sie die Grenze von der Extern- zur Internzone des Varistischen Orogens. Die vielfältige Gesteinsassoziation besteht aus einem Orthogneis-Amphibolit-Komplex, schwach verformten grünschieferfaziellen Sedimenten (?Devon und Unterkarbon) mit überwiegend magmatischem Detritus und einer Reihe verschiedener syn- und postorogener granodioritischer bis granitischer Intrusionen; die gesamte Abfolge wird von spätunterkarbonen Lamprophyren durchschlagen und diskordant von permischen Sedimenten und Vulkaniten überlagert.

Eine coaxiale Gefügeentwicklung während nahezu isothermaler Dekompression im Orthogneiskomplex deutet eine frühe Krustendehnungsgeschichte an. Der Metamorphosehöhepunkt in den anderen Sequenzen (amphibolit-/grünschieferfaziell) während schwacher orogener Verformung wird von einem Blattverschiebungsregime – begleitet von granodioritischen und basaltischen Intrusionen – unter retrograden Bedingungen abgelöst. Der temperaturbetonte Metamorphosetyp, die vorherrschende Blattverschiebungskinematik und die Erhaltung von Teilen der devonisch-karbonischen Sedimenthülle der Kristallinschwelle schließen eine stärkere orogene Krustenverdickung mit nachfolgender Exhumierung aus. Eine Ausnahme bildet wahrscheinlich die unmittelbare Nachbarschaft des Albersweiler Orthogneis und der Burrweiler Schiefer mit ihrer anormalen PT-Geschichte. Die orogene Entwicklung in diesem Teil der Kristallinschwelle wird anscheinend stärker durch thermische als durch Verformungsprozesse gesteuert; dies legt eine wesentliche Rolle der prä- bis postkinematischen Intrusionen nahe.

Die wesentlichen Aspekte der korrelierten Abfolge gefügebildender und thermischer Prozesse legt – auch unter Berücksichtigung der lithologischen Assoziation – das geodynamische Environment eines initialen, submarinen magmatischen Bogens für diesen Teil der Kristallinschwelle nahe. Seine Evolution begann vermutlich während des Oberdevons auf einer zerfallenden kontinentalen Plattform und hielt an während der unterkarbonischen Kollision mit der rhenoherzynischen Zone unter Wechsel des Deformationsmodus der Oberplatte hin zu orogenparallelem Zergleiten.

Abstract

Several small outcrops along the western Rhinegraben escarpment expose rocks which represent the western prolongation of the so-called Mid-German Crystalline Rise. This basement ridge separates the Rhenohercynian and Saxothuringian zones of the Variscan belt of Europe and thus marks the boundary between the external and the internal zones. The variable rock association includes an orthogneiss-amphibolite complex, weakly deformed low grade sediments (?Devonian and Visean), and a number of different syn- to post-orogenic granodioritic to granitic intrusives, all crosscut by Late Lower Car-

*) Authors' addresses: TH. FLÖTTMANN, Department of Geology and Geophysics, The University of Adelaide, Box 498, S.A. 5001, Australia and O. ONCKEN, Geo-Forschungs-Zentrum Potsdam, Telegrafenberg, O-1561 Potsdam/Germany

Manuscript received: 5. 2. 91; accepted: 25. 11. 91

boniferous undeformed lamprophyric dikes and unconformable overlain by Permian sediments and volcanics.

Largely isothermal decompression during coaxial fabric evolution in the orthogneiss complex marks an early stage of deformation possibly due to crustal attenuation. Peak metamorphism (amphibolite/greenschist facies) in the other sequences with only minor orogenic shortening is succeeded by retrogressive strike-slip deformation associated to peak intrusive activity. The encountered typically low-P high-T metamorphism, the predominant strike-slip type kinematic pattern, and the preservation of parts of the Devono-Carboniferous sedimentary cover of the Rise preclude major crustal thickening and subsequent exhumation. An exception is the probably thrust-bounded juxtaposition of the Albersweiler orthogneisses and Burrweiler schists which is supported by their respective PT-paths. The orogenic imprint in the sedimentary cover of the crystalline rise appears to be thermal rather than strain-induced, suggesting a dominant role of the abundant pre- to late-orogenic intrusives.

The essential aspects of this sequence of related structural and thermal events as well as the rock type association suggest a largely submarine incipient magmatic arc type of orogenic environment for this part of the Variscan belt. Its evolution probably started during the Upper Devonian on a disintegrating continental platform and proceeded through the Lower Carboniferous continental collision with the Rhenohercynian zone entailing a concomittant switch in deformation mode of the upper plate.

Résumé

Plusieurs affleurements, situés dans le versant ouest du fossé rhénan, donnent une idée du prolongement occidental du Seuil Cristallin d'Allemagne Centrale («Mitteldeutsche Kristallinschwelle») qui, dans la chaîne varisque européenne, sépare la zone rhénohercynienne de la zone saxo-thuringienne, c'est-à-dire la zone externe de la zone interne des Variscides. L'association lithologique, variée, comporte des orthogneiss à intercalations amphibolitiques, des sédiments (dévoniens à viséens ?) faiblement déformés à facies de schistes verts, provenant surtout de l'érosion de roches magmatiques et d'une série d'intrusions diverses de granites et granodiorites syn- à post-orogéniques. L'ensemble est traversé de dykes lamprophyriques d'âge viséen tardif non déformés et est surmonté en discordance par des sédiments et des volcanites permiens.

Dans le complexe orthogneissique, une déformation coaxiale, concomittante à une décompression presque isothermique, indique une phase initiale de distension de la croûte. Dans les autres séquences (à facies d'amphibolites et de schistes verts), le point culminant du métamorphisme a accompagné une faible contraction orogénique. Ce stade a été suivi d'un régime de décrochement en conditions de rétromorphose, accompagné d'intrusions granodioritiques et basaltiques. Le type de métamorphisme à haute température/basse pression, le cadre cinématique décrochant et la préservation de la couverture sédimentaire dévono-carbonifère du Seuil Cristallin excluent un épaississement majeur de la croûte avec exhumation subséquente. Le voisinage immédiat de l'orthogneiss d'Albersweiler et des schistes de Burrweiler avec leur évolution thermo-barométrique anormale est la seule exception à cette règle. L'évolution orogénique dans cette partie du Seuil Cristallin a été régie davantage par des processus thermiques que par la déformation, ce qui suggère un rôle important des intrusions pré- à post-cinématiques.

Les aspects essentiels de cette histoire où se combinent le développement structural et les événements thermiques, ainsi que l'association lithologique, est caractéristique d'un environnement d'arc magmatique sous-marin pour cette partie de la chaîne varisque. Son évolution a vraisemblablement commencé au Dévonien supérieur sur une plate-forme continentale en voie de désintégration. Elle s'est poursuivie pendant la collision continentale avec la zone rhénohercynienne au Carbonifère inférieur, avec changement du type de déformation de la plaque supérieure en un décrochement parallèle à l'orogène.

Краткое содержание

В западной части рейнского грабена по ряду небольших обнажений установили продолжение среднегерманского кристаллинового порога. Этот порог отмечает границы внешней и внутренней зон варисского орогена, отделяя т.о. реногерцинскую зону от саксонотюрингской. Многообразные ассоциации пород состоят из ортогнейсово-амфиболитного компонента, слабо измененных седиментов зеленосланцевого фация (девон-карбон?) с преобладанием магматического детрита и ряда различных син- и пост-орогенных гранодиоритных до гранитных интрузий; все свиты пронизаны поздними нижнекарбоновыми лампрофиритными дайками и перекрыты несогласно седиментами и вулканитами пермского возраста.

Развитие коаксиальной структуры во время почти-что изотермической декомпрессии в комплексе ортогнейса указывает на расширение порога. За кульминационным пунктом метаморфизма в других свитах (фаций амфиболитов/зеленого сланца), во время слабого орогенного преобразования, последовал сдвиг, сопровождавшийся интрузиями гранодиорита и базальта при ретроградных условиях.

Высокотемпературный метаморфизм, преобладание кинематики сдвига и сохранение части чехла девонско-карбоновых седиментов кристаллинового порога исключают мощное утолщение коры под воздействием процессов орогенеза с последующей эксгумацией. Исключение составляют, вероятно, находящиеся по соседству ортогнейсы Albersweiler'a и сланцы Burrweiler'a с их анормальной термобарометрической историей; развитие орогена в этой части кристаллинового порога, кажется, регулировалось скорее всего термическим воздействием, а не процессами преобразования; именно здесь проявилось в основном влияние до- и пост-кинематических процессов.

Важным пунктом при корреляции последовательности, как термических процессов, так и процессов, образовавших структуры, при учете литологического состава пород является геодинамическая среда исходной подводной магматической дуги в этой части кристаллинового порога. Эволюция его началась, по-видимому, в верхнем девоне на распадающейся материковой платформе и продолжалась во время нижнекарбоновой коллизии ее с реногерцинской зоной, причем модус деформации верхней плиты изменился в сторону распада параллельно орогену.

1. Introduction

Since the work of SCHOLTZ (1930) and BRINKMANN (1948) the so-called Mid-German Crystalline Rise and its early recognized key role within the orogenic framework of the central European Variscides has been a major point of controversial discussion. The alignment of crystalline basement outcrops along the boundary of the Rhenohercynian and Saxothuringian Lower Paleozoic/Devonian basins has led to numerous speculations regarding their age, influence on sedimentation, influence on orogenic fabric formation in the adjoining areas, and, recently, on the inferred plate tectonic setting and role (e.g. WEBER & BEHR, 1983; LORENZ & NICHOLLS, 1984; HOLDER & LEVERIDGE, 1986; MATTE, 1986; OKRUSCH & RICHTER, 1986; ZIEGLER, 1986; FRANKE, 1989; FRANKE & ONCKEN, 1990; KROHE, 1991).

The overall evolutionary pattern of the Mid-European Variscan chain can be summarised to have passed through an initial stage of rifting and basin formation which, however, is not synchronous throughout: The intracontinental Saxothuringian basin opened during the Lower Paleozoic stage of general European crustal stretching and experienced several periods of active volcanism. In contrast the Rhenohercynian continental basin is a late feature which evolved during Devonian times. The oceanic basin intervening between both zones – which is parent to the Giessen nappe pile – probably also has an age no later than Lower/Mid-Devonian (ENGEL et al., 1983; GRÖSSER & DÖRR, 1986). Several authors relate the position of the named basins to a back arc setting above a major N-directed subduction zone evolving in Lower Paleozoic times at the southern border of the Variscan crustal units in the Alpine area (e.g. LEEDER, 1982; ZIEGLER, 1986; MATTE, 1986). The early evolution of the more internal Moldanubian zone and its relationship to the Saxothuringian zone is still unclear. General closure of the Mid-European Variscan basins started during the Early Devonian and was completed in a final collisional stage in the Lower Carboniferous (see MATTE, 1986; ZIEGLER, 1986; FRANKE, 1989 for details).

Within this scenario, the aligned basement units of the Mid-German Crystalline Rise and of its western prolongation, the Normannian High (HOLDER & LEVERIDGE, 1986) are – in spite of complex lateral relationships – at present generally interpreted to reflect the deeply exposed basement of an active margin during Upper Devonian and Lower Carboniferous times (OKRUSCH & RICHTER, 1986; FRANKE, 1989; FRANKE & ONCKEN, 1990; KROHE, 1991; WILLNER et al., 1991; BEHRMANN et al., 1991). This can be also inferred from the juxtaposition of the Rise against the strongly deformed high-P rocks of the Phyllite zone in the southern Rhenish Massif (ANDERLE et al., 1990) – both rock associations forming a paired metamorphic belt (WILLNER et al., 1991) at a S-directed subduction zone with intervening relics of MOR-volcanics (partly preserved in nappes; FLOYD, 1984; GRÖSSER & DÖRR, 1986; MEISL, 1990). Earlier views (until the late seventies) held that the Crystalline Rise was a temporarily emerged parautochthonous basement ridge which shed clastics into the adjacent basins (e.g. BRINKMANN, 1948). Moreover, the rise was also interpreted to have acted as a rigid block during orogenic shortening effecting a bivergent orogenic architecture on either side (SCHOLTZ, 1930).

Apparently, the Mid German Crystalline Rise shows quite contrasting evolutionary patterns east and west of the river Rhine (comp. WEBER, 1990). Due to preservation of parts of the sedimentary cover in the west, as opposed to other parts of the rise, more detailed information on some aspects of the tectonothermal history can be expected in spite of the very restricted number of outcrops (list of outcrops below Fig. 1). The present study focuses on the preextensional (= pre-lamprophyre intrusion, see below) structural and metamorphic evolution of the Paleozoic basement along the western Rhine graben fault (see Fig. 1; ZAMINER, 1957; FRENZEL, 1971); the principal aim is to derive constraints regarding the tectonothermal development of this part of the rise – which may also shed some light on the platetectonic evolution of the entire rise.

2. Geological framework

The generally steeply dipping association of crystalline basement units is essentially characterised by a large number of mostly synorogenic intrusives with calc-alcaline trend (OKRUSCH & RICHTER, 1986; HENES-KLAIBER, 1989; LAU et al., 1990; WILDBERG, 1990). The noncylindrical general structure with a lack of lateral continuity and a rather complex kinematic pattern in part shows barrovian metamorphism (Spessart, Ruhla, Böllstein Odenwald; see OKRUSCH & RICHTER, 1986), in part high-T/low-P metamorphic conditions (Bergstäßer Odenwald; see WILLNER et al., 1991), and – below the Permo-Carboniferous Saar-Nahe basin filling (see below) – may even contain undeformed Devono-Carboniferous sedimentary rocks (HERING & ZIMMERLE, 1976; DONSIMONI, 1981). Radiometric dating (K/Ar on hornblendes, biotites and muscovites) generally yield Upper Devonian to Lower Carboniferous ages (KREUZER & HARRE, 1975; MONTIGNY et al., 1983; LIPPOLT, 1986; NASIR et al., 1991), the timing of peak metamorphism and deformation is still poorly constrained. The essential geological aspects of the western Saxothuringian zone (outcropping areas in Fig. 1) are as follows.

Surface outcrops of the pre-Permian basement constituting the 'Mid German Crystalline Rise' west of the river Rhine are located along the western escarpment of the Rhine graben structure between Neustadt/Weinstraße in the north and Windstein (northern Vosges, France) in the south (Fig. 1). This section of the Mid German Crystalline Rise comprises generally three different rock types; gneisses and amphibolites which crop out at Albersweiler, deformed paleozoic metagraywackes and metapelites with pyroclastic intercalations, and a complex suite of magmatites of dioritic-granitic composition. Earlier work of ZAMINER (1957), FRENZEL (1971), and STELLRECHT (1971) has established the magmatic and metamorphic petrology and some structural aspects of the basement and the metasediments. The composition of the intrusive rocks has recently been examined by LAUE et al. (1990) who established a predominance of subduction-related I-type granitoids.

The basement rocks are dissected by numerous lamprophyre dikes and by Permian basalts ('Melaphyres') which extrude onto a paleo-relief. Lower Permian and Lower Triassic continental clastics unconformably overstep the basement and the extrusive rocks.

Towards the west, the Saar 1 well on the northwestern boundary of the rise has drilled a sequence of Mid-Devonian carbonates passing through the Upper Devonian into a Lower Carboniferous clastics sequence with largely magmatic detritus (total thickness ≈ 1 km). The undeformed and unmetamorphosed sequence overlies a weakly metamorphic granite of poorly constrained Rb-Sr-age (possibly Silurian) and is overlain disconformably by the Westphalian to Lower Permian molasse-type clastic filling of the late-orogenic Saar-Nahe basin (see HERING & ZIMMERLE, 1976; SCHÄFER, 1989, for details).

Towards the southwest, the southern rim of the Saxothuringian zone in the northern Vosges (Val de Bruche) contains a more flysch-type, and strongly deformed sedimentary sequence of more than 1.5 km in thickness compositionally similar to the Saar 1. This clastics series is completed by the Lower Carboniferous volcanic sequence of Schirmeck (see JUTEAU, 1971; WICKERT & EISBACHER, 1988). Accompanying Lower Paleozoic finegrained clastics are also found in the northernmost Black Forest (WICKERT et al., 1990). The sedimentary rocks are

Fig. 1. Geological sketch map of Upper Rhine graben area showing rock distribution of western Mid German Crystalline Rise in outcrops and bore holes; small inset shows position of study area within the Variscan framework; large numbers refer to sequences analysed in the present paper: 1 – gneiss basement; 2 – medium-grade metasediments; 3 – granitoids; 4 – low-grade metasediments. ►

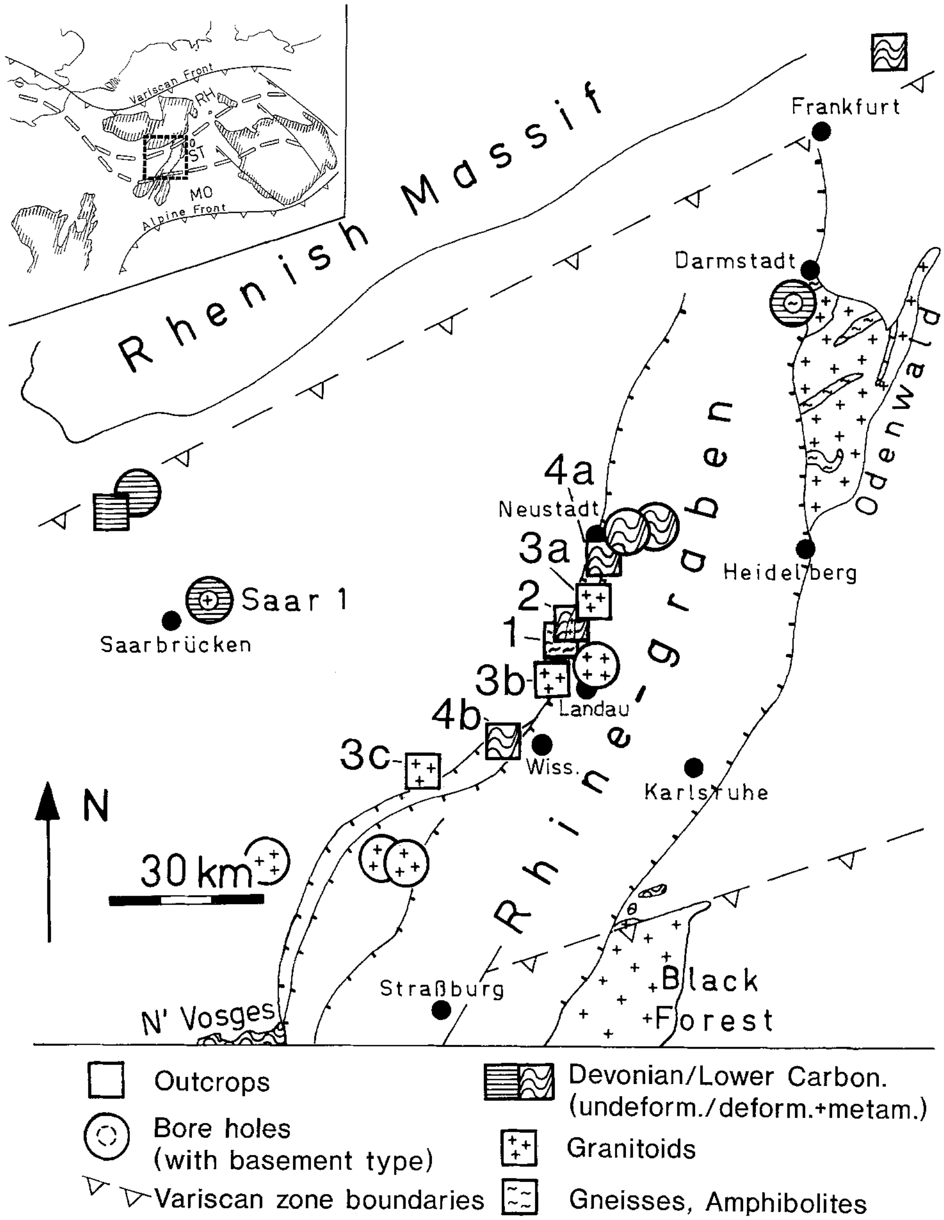

List of outcrops

Nr. in Fig. 1	rock type	outcrop	r	h
			(Gauss-Krüger-coordinates)	
1	gneisses	Albersweiler		
	amphibol.	north. quarry	3428800	5454150
	lamproph.	south. quarry	3428700	5453800
2	metapelites	Burrweiler	3432600	5458450
3a	granite	Edenkoben east	3434050	5460880
		west	3433730	5460950
3b	granodiorite	Kaiserbachtal	3427300	5447700
4a	metagraywack.	Neustadt	3436520	5468900
		Hambach	3436160	5466840
4b		Weiler/Germannshof	3419950	5434550
3c	granodiorite	Windstein (Elsaß) roadside outcrops along D53 between Windstein and Wineckerthal in Schwarzbach-valley northwest of Jaegertal		

intruded by predominantly calc-alcaline I-type plutons (WILDBERG, 1990) which may also show some deformation (comp. WICKERT & EISBACHER, 1988; WICKERT et al., 1990). Metamorphism in this sequence reaches lower greenschist conditions in the south and decreases to the north. The kinematics are governed by earlier thrusting outlasted by strike-slip faulting.

Contrary to the evolution west of the river Rhine, the Odenwald mountains forming the eastern graben shoulder (Fig. 1) lack well-dated and undeformed sediments. The deeper exposed basement largely consists of syn- to late-orogenic calc-alcaline intrusions (HENES-KLAIBER, 1989) into a previously metamorphosed volcanic and sedimentary sequence which essentially experienced high-T/low-P conditions with some slivers yielding an earlier P-dominated imprint (OKRUSCH et al., 1975; KROHE, 1991; WILLNER et al., 1991). The kinematic pattern within the steeply dipping series is largely controlled by syn-intrusive strike-slip movements which subdivide the Odenwald into a number of units with different tectonothermal evolution (KROHE, 1991). The gabbro-granite intrusive assemblage yields cooling ages between 360 and 330 Ma. Indication of some earlier hornblende ages (ca. 370 Ma) in the meta-volcanics/-sediments (KREUZER & HARRE, 1975; KIRSCH et al., 1988) suggest an earlier synorogenic (?) metamorphic overprinting.

3. Geology

3.1. Basement at Albersweiler

3.1.1. Metamorphic rocks

The crystalline basement is exposed in a quarry complex near Albersweiler (1 in Fig. 1; Fig. 2a; the structural and petrological inventory has in part been described by ZAMINER, 1957, and STELLRECHT, 1971). The predominant rock type is a heterogeneously layered (m-scale) gneiss (minimum thickness: 500 m) containing on average 10% biotite and plagioclase + quartz + K-feldspar at roughly equal amounts, and hornblende in some layers. K-Ar data on biotite by FRENZEL (1971) yield – considering modern decay constants – about 340 Ma. Alternating biotite and quartz-feldspar layers of 1 cm to several centimetres thickness form a S-dipping metamorphic foliation of variable intensity (depending on biotite content) which is the principal gneissic fabric (Fig. 2c). The leucocratic minerals are elongate in the foliation (aspect ratios up to 1:3). Undulatory extinction, deformation lamellae and subgrain formation (in quartz, feldspar, biotite) indicate crystal plastic deformation.

In the northern, structurally deeper part, the gneisses show intercalations of amphibolite lenses and pods. The amphibolite/gneiss contacts are often obliquely oriented to the foliation (Fig. 2b). The amphibolites are only crudely foliated and show mineral assemblages of quartz + plagioclase + hornblende + biotite or plagioclase + hornblende + titanite + epidote synkinematically stable to the foliation. Hornblende is undulatory and may be twinned, plagioclase shows deformation twins, subgrains and incipient recrystallization. A postkinematic disequilibrium mineral assemblage consists of unstrained hornblende overgrowths with plagioclase + epidote + titanite + chlorite (Fig. 2d).

Aplites containing quartz + plagioclase + K-feldspar at roughly equal amounts ± biotite intruded the basement syn- (biotite-rich) to latekinematically (no biotite; Fig. 2b, c) with respect to the foliation. Late- to postkinematic aplites and pegmatites in places enclose gneiss rafts, giving rise to an agmatic schollen structure.

In the abandoned southern quarry, plagioclase and K-feldspar show extensive post-foliation grain growth (diameter up to 6 mm) which gives rise to a massive, metablastic rock texture (Fig. 2e, f). Cores of plagioclase blasts have average An-contents of 23 mol%, An-contents in the rim scatter around 20 mol%. Muscovite grew concomittantly (Fig. 2f) at the expense of all mineral phases. The grain boundaries of the postkinematic assemblage plagioclase

Fig. 2. Rock types at Albersweiler northern quarry; a) western wall of quarry showing abundant lamprophyric dikes crosscutting the gneiss, both overlain by subhorizontal Permian sediments (in trees); b) complex gneiss-amphibolite contact suggesting overprinted intrusive nature with numerous deformed aplitic veins; c) polished hand specimen of biotite-rich foliated gneiss with amphibolite layers and three generations of synkinematic aplite veins, the final system (A3) evolving from incipient melting along contemporaneously forming microcracks subperpendicular to foliation, earlier A2 is fully developed and folded tightly, while A1 is already entirely rotated subparallel to foliation; d) micrograph from amphibolite showing hornblende (H) with postkinematic actinolitic overgrowths, plagioclase (P), and epidote (E); e) gneiss with metablastic texture obliterating the foliation due to plagioclase grain growth; f) micrograph of metablastic texture with large plagioclase (centre) overgrowing biotite (dark) and quartz, muscovite grows from biotite and along grain boundaries (arrows), quartz has lobate grain boundaries; g + h) kersanitic lamprophyre in contact with metablastic gneiss showing late crack-seal calcite veins and magmatic flow fabric along contact formed by pervasive orientation of retrogressed mineral assemblage (mostly chlorite). Micrographs d, f, h with crossed nicols; white scale bar is 0.5 mm, scale bar in c, g is 1 cm. ▶

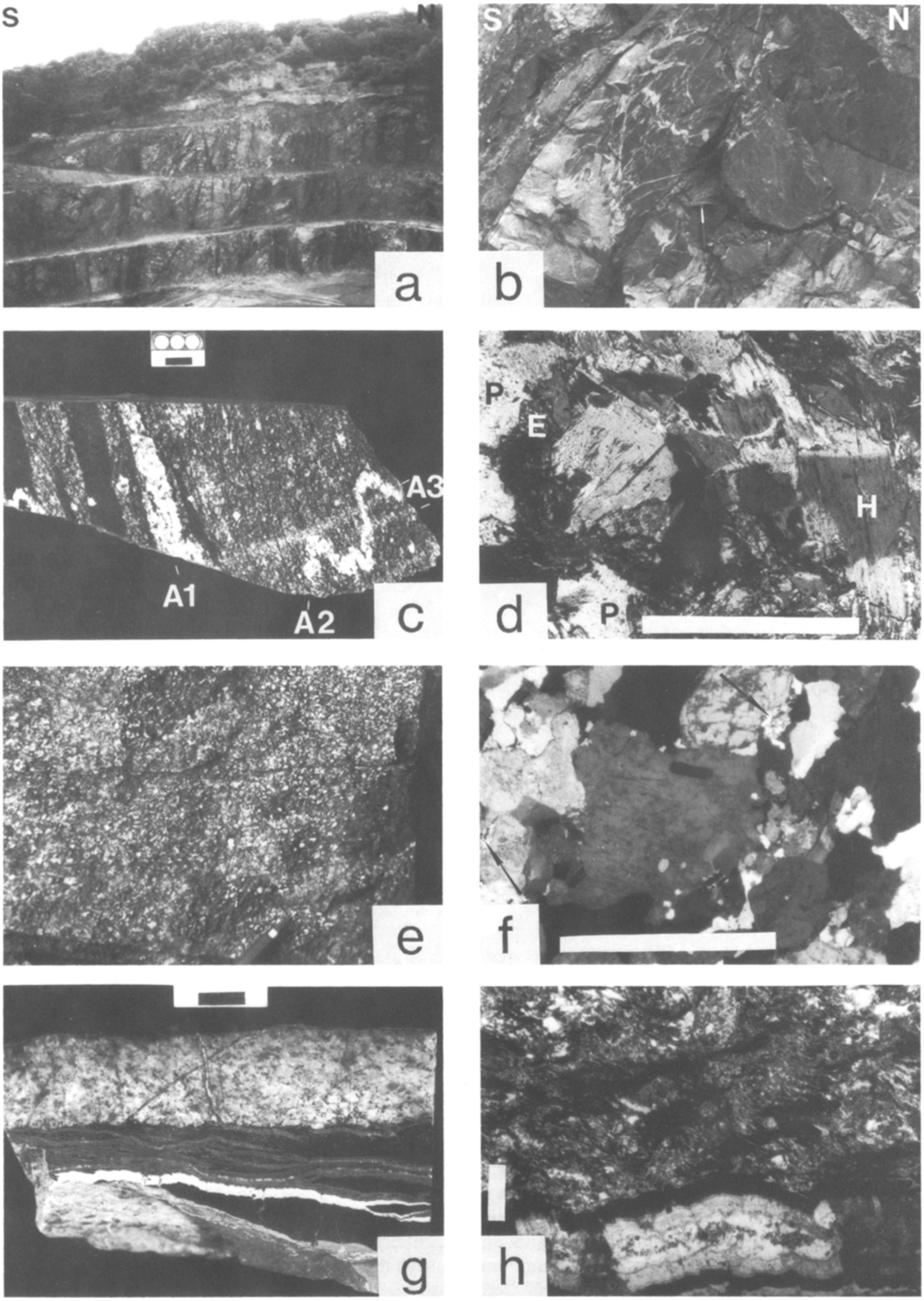
S
N
a
S
N
b
A1
A2
A3
c
P
E
H
P
d
e
f
g
h

+ K-feldspar + muscovite + quartz ± biotite are straight or embayed.

3.1.2. Basaltic rocks

The basement is intruded by 4 dike generations, all of grossly basaltic composition (FRENZEL, 1971; LAUE et al., 1990). The oldest generation (I; in northern quarry wall) strikes N-S. The primary fabric is often overprinted by intense ductile shear deformation at very low grade conditions along wrench faults (see below). A second generation of basaltic dikes (II) with minor brittle deformation strikes W-E and is of spessartitic composition (FRENZEL, 1971): The mineralogy is governed by strongly altered plagioclase phenocrysts (An > 40 mol%) of up to 3 cm in diameter which are encrusted by a second, unaltered plagioclase generation (An = 10 mol%), and by equigranular hornblende grains (diameter 0,5 cm) with magnetite cores often overgrown by fibres of actinolitic hornblende. Magnetite is stable with the first hornblende and plagioclase generation, whereas together with the second hornblende and plagioclase generation also chlorite, muscovite, and ± epidote occur.

The third ubiquitous, undeformed generation of basaltic dikes (III) are brownish kersantitic lamprophyres with minor amounts of hornblende (FRENZEL, 1971), which also strike W-E (Fig. 2a, g, h). K-Ar data by FRENZEL (1971) on Biotite and hornblende from this generation give – considering modern decay constants – 330 Ma. Associated with these late lamprophyres are extensional veins filled with unoriented calcite and opaques. A later vein generation is filled with calcite only. Both vein types occur within the lamprophyres and extend into the basement. The veins have crack-seal deformation character (RAMSAY, 1980, Fig. 2h), suggesting high pore pressures during and after lamprophyre emplacement. The lamprophyre intrusions are followed by basaltic extrusives ('Melaphyres', IV), which form flow units on a distinct paleo-relief.

3.1.3. Structures and kinematics

The oldest structural element is the S-dipping gneiss foliation. The synkinematic aplitic dikes, oriented normal to the foliation are symmetrically folded around E-W trending axes (Fig. 3e). The nearly rhombic fold geometry and the absence of a lineation and of a preferential porphyroclast asymmetry suggest bulk coaxial flattening during the formation of the gneiss foliation (see Fig. 2b, c).

The gneiss foliation is crosscut or reactivated by ductile, mostly E-W striking mylonite zones (Mylonite I), which dip to the S (Fig. 5a). The mylonites show a marked concentration of fine-grained biotite (25%) + muscovite + chlorite, and plagioclase (50%) ± calcite and have sharp contacts with the country rock (Fig. 4a, b, c). In some places it can be observed that the mylonites developed from retrogression of previously boudinaged amphibolites (Fig. 4a). The deformational sequence (boudinage – mylonitization) stipulates a reaction-enhanced reversal of the relative strengths from 'stiff' amphibolites to 'weak' biotite or chlorite schists resulting in a strain localization in the biotite-chlorite mylonites. Oblique E-directed displacement of the hangingwalls is indicated by asymmetric porphyroclasts of metablastic gneiss and feldspar (Fig. 4b) and an s-c fabric in combination with a subhorizontal WSW-trending mineral elongation lineation, developed on the mylonitic surfaces. Quartz is elongated, the recrystallizate has stable grain boundaries. Plagioclase with deformation lamellae and subgrains is stretched (aspect ratios up to 1:4) asymmetrically to the foliation. The recrystallised grains have stable mutual grain boundaries also with quartz and biotite (Fig. 4c) which grew in the plagioclase pressure shadows. Chlorite, muscovite, and calcite grew late- to postkinematically from biotite and hornblende.

This mylonite type shows abundant chlorite coated microcracks in quartz which are oriented perpendicular to the mylonitic foliation (c-planes). The s-planes are marked by carbonate-filled, late-kinematic crack-seal veins which in places are cut through by the c-planes. The intense sealed micro-faulting indicates increased pore pressures during mylonitization and a dominant role of fluid-influx resulting in a reaction-enhanced strain-softening. The mica mylonites are crosscut by the first generation basaltic intrusives (Fig. 7).

Subvertical N-S trending, 1–4 metres thick mylonite zones (Mylonite II, preserved in northern quarry wall) consist of penetratively deformed gneisses and of first generation basaltic intrusives with a subhorizontal mineral stretching lineation (Fig. 4d). Offsprings of these mylonite zones crosscut the biotite-mylonites. The gneiss-mylonites consist of quartz and sericite which are asymmetrically deflected in s-c fashion. Quartz forms asymmetrically elongated ribbon grains with a markedly crystallographic preferred orientation. Quartz subgrains have sutured grain boundaries (Fig. 4f). Locally subgrain misorientation leads to

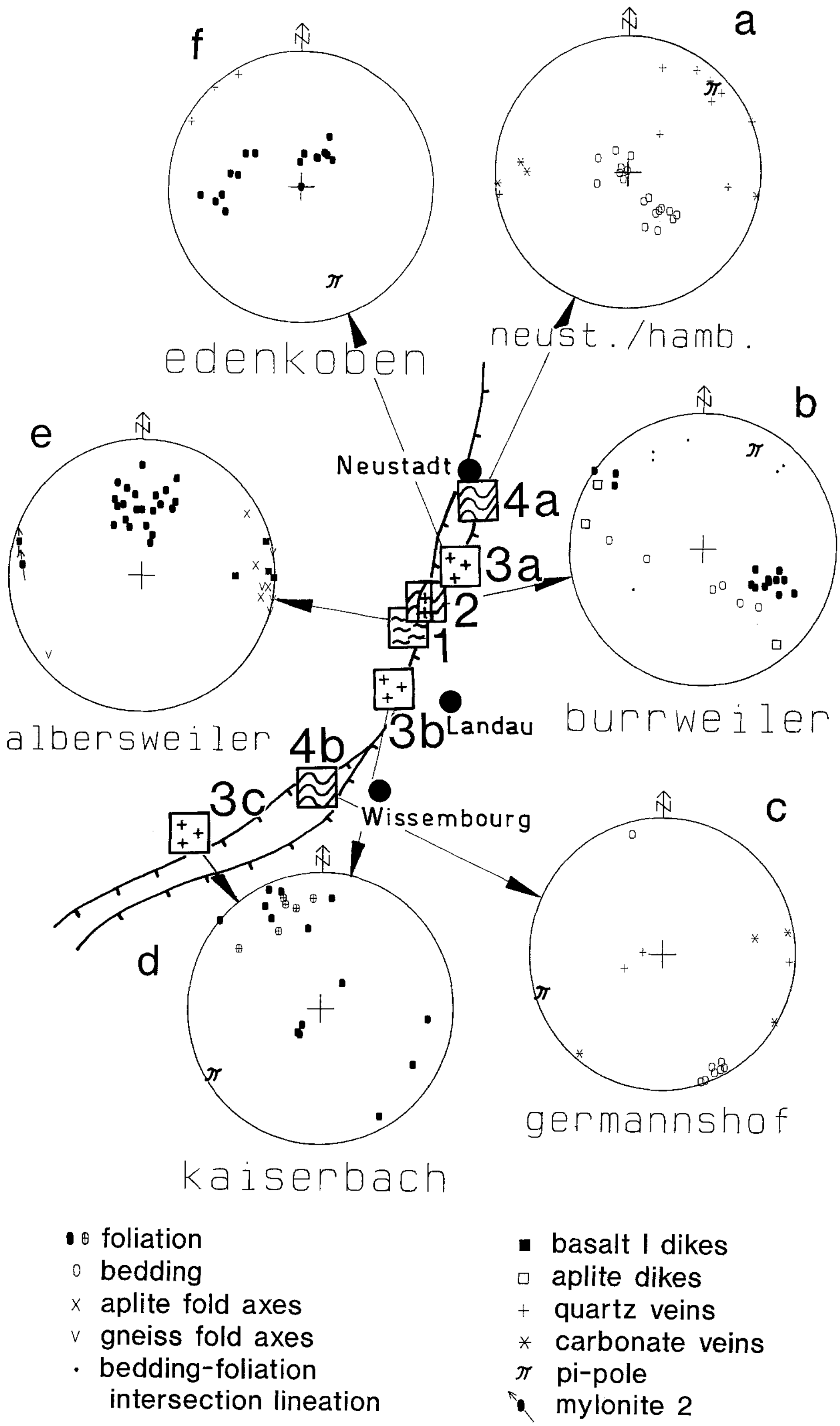

Fig. 3. Macrofabric in analysed sequences in lower hemisphere equal area projection; outcrop numbers refer to identical numbers in Fig. 1 and outcrop list in appendix; foliation includes metamorphic (b, e) and magmatic foliation (d, f); in d filled black circles indicate magmatic foliation, open crossed circles are metamorphic foliation in enclosed amphibolite body.

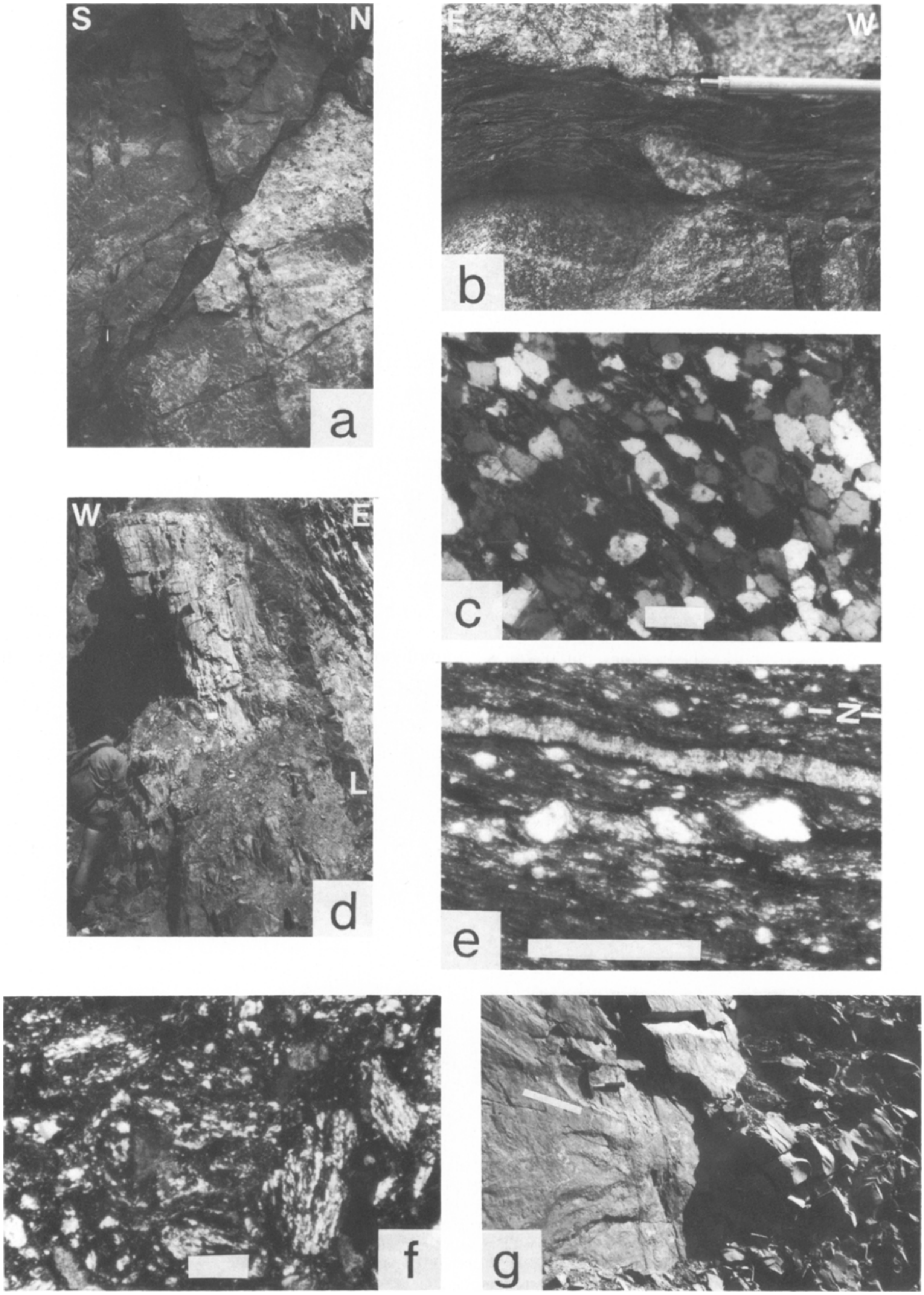
S
N
a
E
W
b
c
W
E
L
d
Z
e
f
g

the formation of independent quartz grains indicating rotation recrystallization. The mylonitised basaltic rocks consist of 85 % strongly oriented and intimately intergrown sericite/chlorite with minor muscovite and opaques. Sigma and delta quartz clasts (Fig. 4e) and the s-c fabrics show sinistral strike slip displacement along the faults. Opaques and chlorite grew in the pressure shadows and at quartz grain boundaries, indicating the contribution of diffusion controlled deformation processes. Weakly developed shear bands with synkinematically grown chlorite deflect the mylonite foliation and indicate a consistent sense of displacement. Muscovite and chlorite are stable postkinematically.

The mylonite II-fabric is overprinted by discrete cataclastic microfaults which coagulate to form a cataclastic network made up by angular quartz grains, opaques, sericite, and chlorite. The cataclasites contain fragments of the previously formed mylonites (Fig. 4f). Both, mylonites and cataclasites are crosscut by cracks with antitaxially grown carbonate oriented subperpendicular to the mylonite foliation. The N-S trending fault zones are dissected by the roughly W-E trending spessartitic basalts (generation II). Small, centimetre thick epidote filled veins in the basement show similar crosscutting relationships.

The mentioned brittle shear zones cut the N-S trending mylonites, dike generations I and II, and the epidote veins. They form a conjugate set with horizontal slickensides indicating compression with along-strike extension (Fig. 4a, g). The dextral E-W trending strike slip zones are intruded by postkinematic lamprophyre dikes III (Fig. 4g), which are deformed by normal faults only.

3.1.4. Metamorphic evolution

The Albersweiler gneiss and amphibolite assemblage was vaguely interpreted to be of sedimentary origin with later granite intrusions (ZAMINER, 1957). However, in the view of LAUE et al. (1990) the mineral assemblage in the gneisses and their geochemical fingerprint rather suggest a

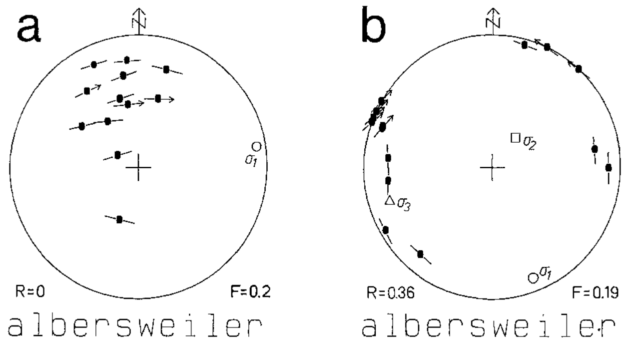

Fig. 5. Fault kinematics at Albersweiler; lower hemisphere equal area plots show mylonite I in a and late brittle strike-slip faults in b; black circles are poles to the faults, lines trace the common great circle of fault pole and striation/stretching lineation, arrow shows sense of slip of hangingwall (projection method from HOEPPENER, 1955); equally shown are computed axes of deviatoric stress tensors, the shape factor of the tensors (R) and the fluctuation of the fault populations (F; see ETCHECOPAR et al., 1981, and ONCKEN, 1988, for method).

magmatic protolith. The often discordant character of the gneiss amphibolite contacts with the regional foliation (Fig. 2b) indicates that the amphibolites originated from intrusions into the gneiss protolith prior to regional deformation and metamorphism. For the synkinematically stable assemblages in the amphibolites and in the hornblende-gneisses the geothermo-barometer of PLYUSNINA (1982) gives pressures of 3–4 kb at temperatures around 540 °C (data see table 1). The temperatures obtained by using the plagioclase-hornblende geothermometer of SPEAR (1980) are somewhat lower around 520–490 °C. The aplitic veins in the basement, however, are at least initially of minimum granite eutectic composition suggesting that partial melting took place. Therefore the thermal calculations based essentially on the An-content in feldspars most probably do not reflect peak metamorphic conditions but rather are subject to late-/postkinematic re-equilibration and feldspar blastesis – the calculated temperature thus probably are minimum values.

For the postkinematic mineral assemblage in the amphibolites (recrystallized plagioclase rims and hornblende overgrowths) temperatures were around

◄ **Fig. 4.** Faulting at Albersweiler; a) boudinaged amphibolite retrogressed to a chlorite schist with motion top to the E, crosscut by a late dextral strike-slip fault; b) biotite mylonite of same generation formed from amphibolite layer with σ-clast of metablastic gneiss; c) microfabric of mylonite in 4 b with equigranular strain-free quartz and plagioclase grains with equilibrated grain boundaries and well oriented oxidised and sericitised biotite; d) sinistral strike slip mylonite II zone crosscut by undeformed kersanitic lamprophyre (L = basalt III); e) micrograph of mylonite II fabric in basalt I with chlorite (matrix) and quartz- σ- and δ-clasts indicating sinistral shear, orientation of thin section is subhorizontal (N to the right), late basalt II-related calcite vein cuts mylonite; f) cataclasite from brittle strike-slip fault crossing mylonite in 4d (right side of lamprophyre) showing mylonitic clasts with well developed low-temperature quartz fabric; g) late strike-slip fault (white bar shows orientation of slip) in gneiss intruded by basalt III dike (right). All micrographs with crossed nicolls; white scale bar is 0.5 mm in c, f and 0.2 mm in e.

520 °C at pressures of 2 kb. Also, the postkinematic feldspar blastesis with the concomittant muscovite stability and the absence of partial melts during this stage indicate static tempering at upper greenschist facies conditions (Fig. 6).

In some of the generation I mylonites synkinematic biotite + muscovite + plagioclase + quartz are stable, indicating temperatures in excess of 420 °C for initial mylonitization (SPEAR & CHENEY, 1989). Locally, synkinematic chlorite/sericite stability indicates that the faults of this structural episode were also active at lower temperatures (below biotite isograd). Probably, the above mentioned biotite ages record cooling through this stage.

In the mylonite II generations (N-S trending strike slip faults), synkinematic quartz and sericite stability and the quartz texture (recrystallization and unequilibrated grain boundaries) indicate synkinematic temperatures around 300 °C (VOLL, 1976). Subsequent cataclastic overprinting is outlasted by muscovite chlorite stability, indicative of very low grade metamorphic conditions during this stage. In the basalts crosscutting the N-S trending ductile faults (basalt II), hornblende Al-barometry (HAMMARSTROM & ZEN, 1986) indicates an intrusion depth of equivalent to < 1 kb pressure (< 3 km) for the basalts. The P-T-D path derived from these relationships and from the structural data is given in Fig. 6.

On the whole, the Albersweiler gneisses lack any signs of higher pressure metamorphism. It is thus concluded that peak metamorphism was of low pressure/high temperature type followed by nearly isothermal exhumation during pervasive coaxial deformation and subsequent cooling at very elevated geothermal gradients. During this final cooling stage the basement went through a succession of structural and magmatic events: mylonite I (top to the east) − > basalt I + mylonite II (strike-slip) − > basalt II + cataclasis (strike-slip) − > basalt III (weak N-S extension) − > basalt IV (comp. Fig. 7).

3.2. Metasedimentary rocks

3.2.1. Metapelites at Burrweiler

Near Burrweiler (2 in Fig. 1) finegrained metasediments are exposed with a partly preserved sedimentary fabric. The several 10 m thick sequence predominantly consists of pelites with minor thin (mm-scale) intercalations of silty, quartzitic to arcosic layers and some tuffaceous layers (comp. ZAMINER, 1957). The few unrecrystallized quartz grains and the seriticised plagioclase grains are subangular to well rounded with sizes below 0.5 mm (Fig. 8b). The metasediments are intruded by several aplitic dikes (S-type according to LAUE et al., 1990) during late stage deformation. According to ILLIES

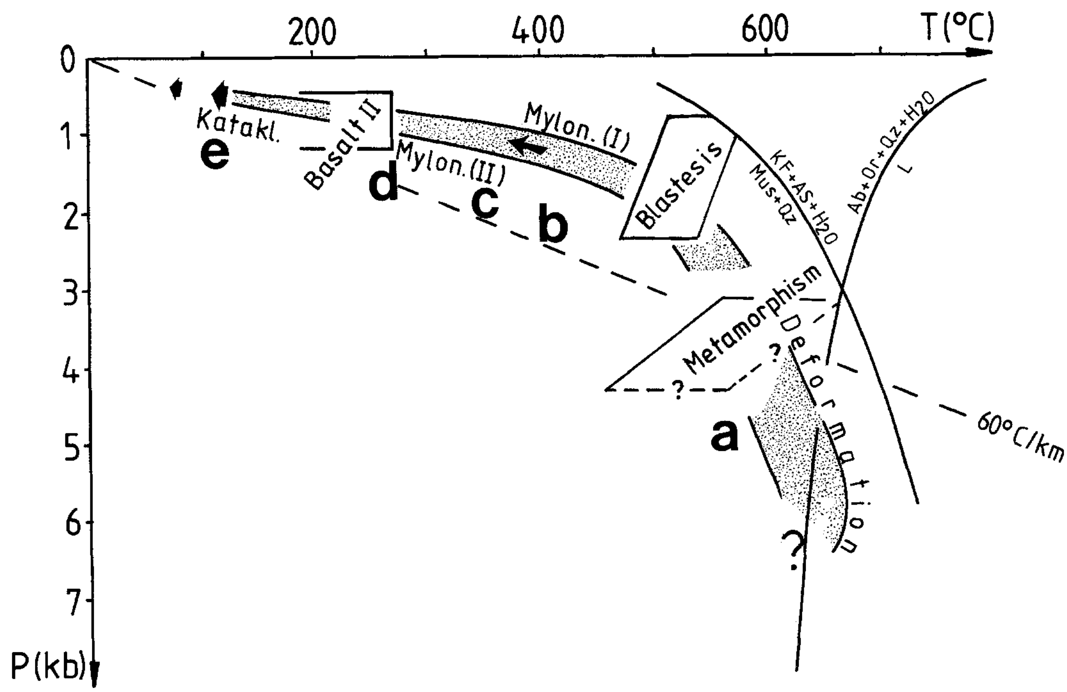

Fig. 6. P-T-D path of Albersweiler gneiss complex; see text for discussion, source of data, and thermobarometric analysis. Letters a to e refer to deformational stages shown in Fig. 7.

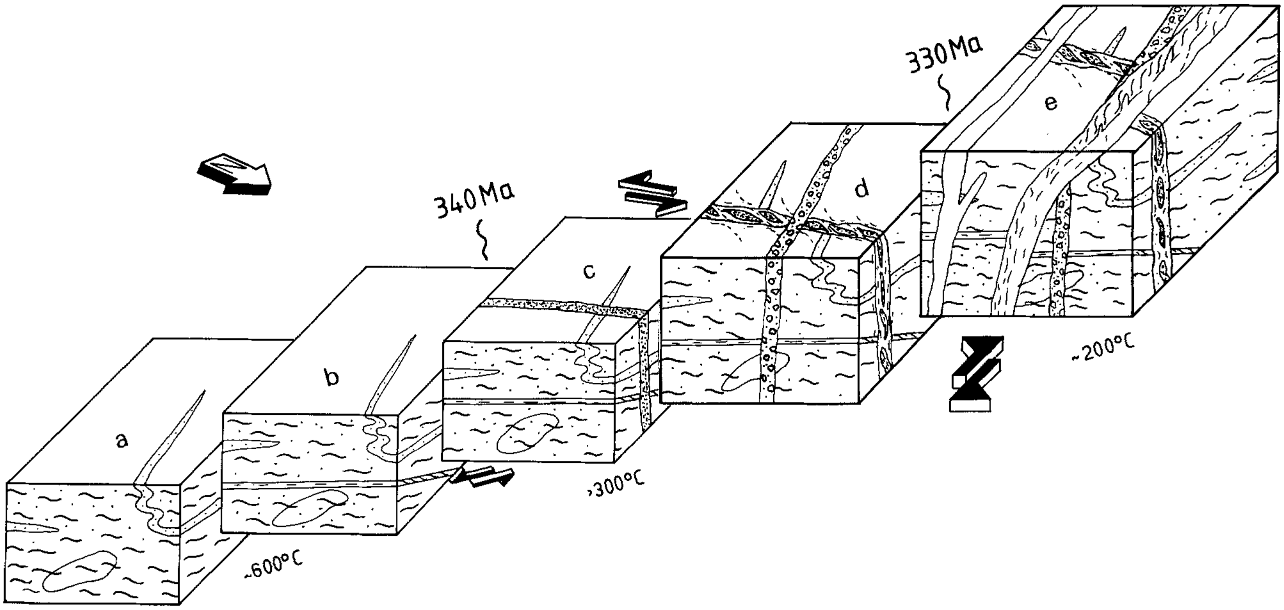

Fig. 7. Sketch of structural evolution of Albersweiler gneiss complex; a) peak metamorphic fabric formation with synkinematic aplites; b) mylonite I formation (biotite-chlorite schists) after metablastic stage; c) intrusion of basalt I generation; d) mylonite II formation with strike-slip motion and intrusion of basalt II generation followed by quartz- and epidote-filled veining; e) brittle strike-slip faulting and final intrusion of basalt III generation (kersantitic lamprophyres). Age data from FRENZEL (1971) and approximate temperatures are tentatively included (comp. Fig. 6).

(1963) the abundance of microgranite pebbles in the Permian conglomerates overlying the Burrweiler sequence increases to the north and merges with the outcropping Edenkoben granite (see below). The age of the sequence is unclear; comparison with well dated sediments in the Val de Bruche in the northern Vosges (JUTEAU, 1971), the Saar 1 well (HERING & ZIMMERLE, 1976), and nearby metasediments at Weiler and Neustadt (see below) suggest a post-Mid-Devonian age of sedimentation, but do not rule out an Early Paleozoic age.

The macrofabric is controlled by a moderate NW- to steep SE-dip of the fabric (bedding parallel cleavage). Some small, nearly isoclinal folds affect bedding as well as early thin quartz veins; the axes dip N to NE (Figs. 3b, 8c, e). The differences along the small outcrops suggest some late rotation, possibly along Rhine graben-parallel faults. Only one pervasive cleavage is formed by preferred alignment of mica and porphyroblast pressure shadows in the generally weakly deformed rocks (Fig. 8e). Cataclastic deformation with formation of dolomite- and chlorite-filled veins is weak and mainly restricted to the aplitic dikes and their immediate vicinity.

The rock composition is dominated by biotite ($\geq$70% in pelitic, $\geq$ 30% in psammitic layers) + quartz + muscovite (~ 10%) + opaques and graphite.

Texture and growth relationships suggest a differentiated tectonothermal evolution: A rare early assemblage in metapelites of quartz + biotite + cordierite (largely retrogressed) + K-feldspar (only established by diffractometric analysis) points to pre- or early-kinematic high-T/low-P conditions (Fig. 8a, c). Retrogression results in breakdown of cordierite to first biotite, then biotite + muscovite, both products growing in the cordierites and in pressure shadows parallel to the cleavage (Fig. 8d). Psammitic layers may show quartz + garnet (unzoned, ca. 80 mol% almandine) + some s_1-parallel biotite in unconspicuous pressure shadows (Fig. 8f). Biotite mostly is decomposed to hematite + muscovite $\pm$ chlorite, the latter two growing epitactically on the biotite lattice. All phases generally show equilibrium grain boundaries and are devoid of crystal-plastic strain; biotite and quartz have recrystallized extensively, the latter showing stable triple junctions (Fig. 8f, g). Unoriented growth of large undeformed muscovite porphyroblasts (up to 5 mm) $\pm$ chlorite at the expense of the biotite-sericite intergrowth overprints the entire fabric (Fig. 8g). An unidentified unoriented fibrous brownish phase near the contact to the aplitic dikes equally overgrows all earlier phases.

The aplitic dikes consist of quartz (15%) + K-feldspar (40%) + plagioclase (20%) + muscovite (15%) and some opaques. All phases are strongly

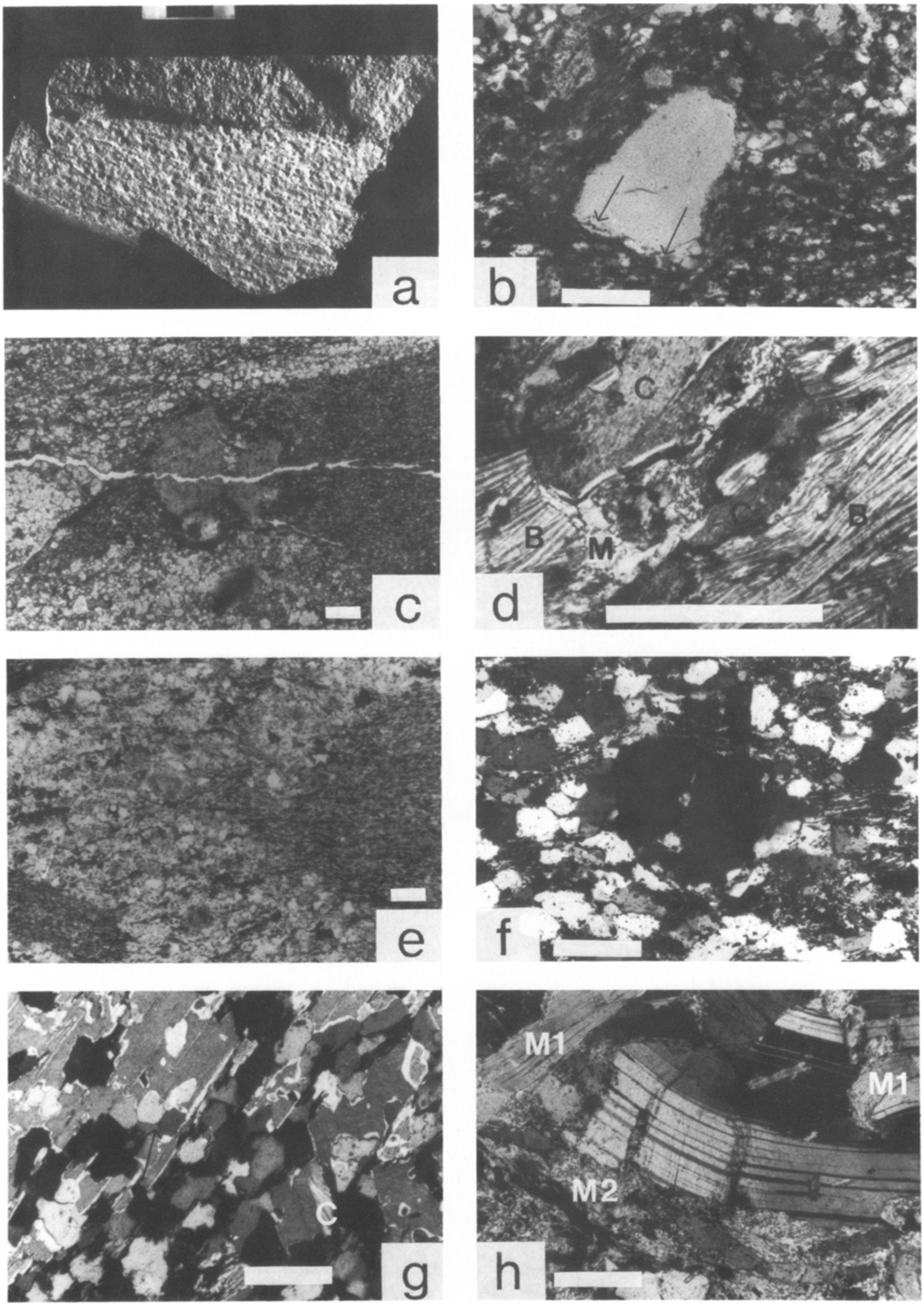
a
b
c
B
M
C
B
c
d
e
f
c
g
M1
M1
M2
h

deformed showing fracturing, undulose extinction, and deformation lamellae. Especially muscovite disintegrated into a small secondary sericite phase (Fig. 8b). The fabric is not recovered – apart from some subgrain formation in quartz – and, on a macroscopic scale, is associated to plagioclase-filled veins and localized brittle strike slip faults absent in the nearby metasediments.

Construction of a PT-path relies on the observed textural relationships and is based on petrographic associations as well as on thermobarometric data on the early equilibrium and the late disequilibrium assemblages (biotite-garnet-thermometry according to FERRY & SPEAR, 1978 and SPEAR & CHENEY, 1989, phengite-barometry according to MASSONNE & SCHREYER, 1987; see appendix for details). Peak thermal conditions were obviously reached during early- or pre-kinematic times (Cordierite + K-spar!). Reconstructed synkinematic conditions (garnet + biotite) only yield minimum temperatures with the FERRY & SPEAR thermometer (1978) due to the compositional change of biotite during breakdown to muscovite + hematite. The Fe/(Fe+Mg) ratio (see SPEAR & CHENEY, 1989) of garnet coexisting with biotite gives ca. 550 °C at the calculated pressures: biotite-phengite intergrowths from the synkinematic cordierite breakdown give Si-contents of 3.2-3.3 (p.f.u.), equivalent to 6–8 kbs at the above temperatures. Evidence for the contemporaneous formation of the two mentioned synkinematic parageneses is indirect which limits the reliability of the above PT-values. However, the very uniform composition of both, garnets and phengites (see appendix), the lack of a zonation, and their contemporaneousness to the foliation are interpreted to support their strictly synkinematic formation.

The disequilibrium assemblage of postkinematic muscovite + biotite ± chlorite + well-equilibrated quartz with stable triple junctions points to lower greenschist facies conditions at decreasing pressures (Si = 3.1–3.2 p.f.u.). Due to the absence of Fe-Mg silicates and due to a 10–20% paragonite solid solution in the phengites, the aplitic phengites, with Si = 3.05–3.1 (p.f.u.), do not yield usable pressure data; the phengites, moreover, possibly rather reflect the brittle deformation stage since most white micas are strongly fractured during the very low grade conditions.

Curiously, the PT-evolution follows a rather unusual path with the peak temperature at an earlier stage and the peak pressure reached during succeeding deformation (Fig. 9). Obviously, the early low-P/high-T imprint must be related to heating prior to a tectonic stacking and deformation event-possibly in the environment of a contact aureole of an early intrusion. Late cooling and concomittant decompression are not accompanied by deformation until the final emplacement of granitic melts at shallow depths. Cataclasis with hydraulic fracturing and strike-slip motion appears to be partly related to this late stage intrusion, in part possibly to the later, Cenozoic Rhinegraben tectonics.

3.2.2. Metagraywackes at Neustadt and Hambach

On the flanks of the Speyerbach-valley in the western outskirts of Neustadt, and at Hambach (4a in Fig. 1) minor outcrops of metagraywackes and shales (ZAMINER, 1957) are unconformably overlain by Lower Permian continental clastics. Plant and trace fossils described by MÜNZING (1956) and by HÄNTZSCHEL (1972) point to an Early Lower Carboniferous age of the graywackes (thicknes ≥ several 10 m). The rocks are medium- to fine-grained (≤ 3 mm), and are mainly composed of partly corroded quartz, some sedimentary fragments (cherts, shale), plagioclase (sometimes zoned), K-feldspar, some white mica and heavy minerals. Magmatic detritus is the main component besides sedimentary fragments; metamorphic detritus is absent. The components are generally poorly rounded or subangular, sorting is weak. Bed thickness varies between some 10 cm and 1 m, sometimes cut by channels (Fig. 10a). Most beds show incomplete Bouma cycles (layer A often missing) with graded bedding. Internal sedimentary features include weak sole marks (mostly load casts), an unlayered part at the base of the

◄ **Fig. 8.** Petrography and fabrics in Burrweiler schists; a) biotite schist with abundant retrogressed cordierite porphyroblasts; b) detrital, rounded quartz grain with overgrowths shown by dust-traced former outline (arrows) in largely recrystallised matrix; c) cordierite porphyroblast – nearly entirely retrogressed – with biotite pressure shadows in metapelite with quartzitic intercalations; d) detail from 4c (lower centre) showing cordierite relic (C) breaking down to biotite (B) and muscovite (M) both growing parallel to the cleavage; e) tight B1-fold of thin quartzitic intercalation with axial planar cleavage formed by aligned newly grown biotite; f) almandine-rich garnet in quartz-biotite schist with unconspicuous pressure shadows, equilibrated quartz texture, and largely decomposed biotite (to hematite and muscovite); g) exaggerated postkinematic muscovite grain growth (± chlorite, C) enclosing equilibrated quartz texture with stable grain boundaries and triple junctions (arrow); h) aplite with quartz, plagioclase showing bent deformation twins (kinked inclusion trails), and deformed magmatic muscovite (M1) disintegrating into a cataclastic finegrained sericite (M2). b, d, f, g, h with crossed nicols; scale bar in a is 1 cm, and 0.2 mm in all other micrographs.

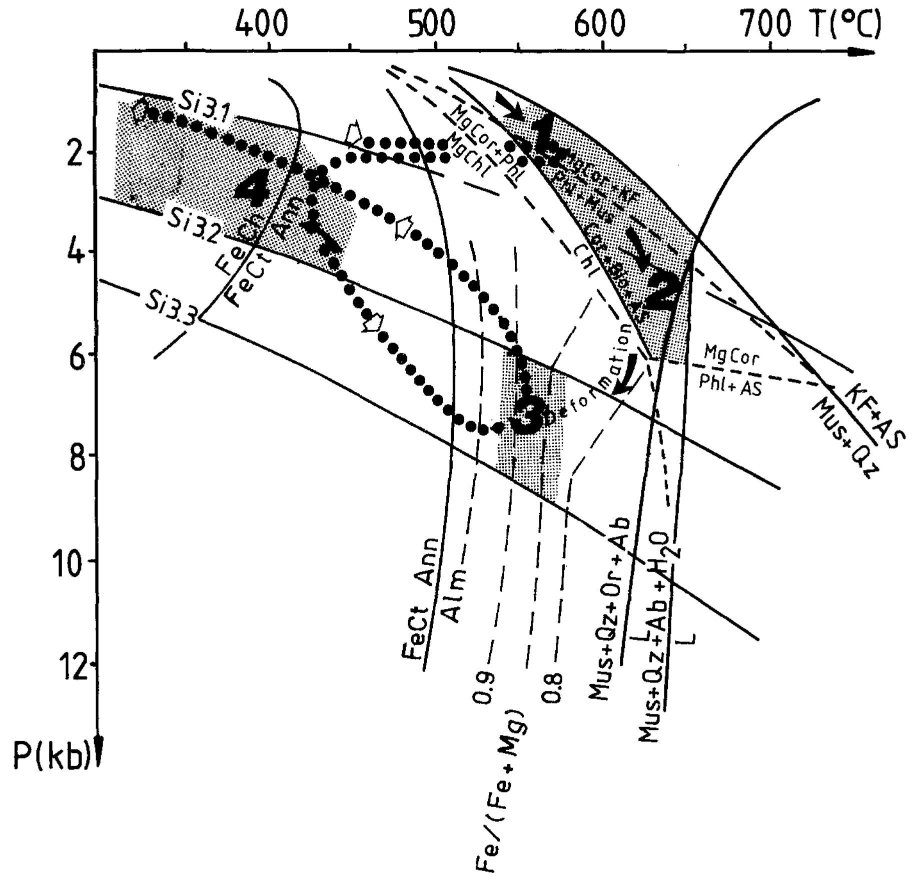

Fig. 9. P-T-D path of Burrweiler schists; reaction isograds and Fe/(Fe+Mg)-isopleths for garnets in biotite-bearing assemblages are from SPEAR & CHENEY (1989), Si-isopleths from MASSONNE & SCHREYER (1987); P-T-stages 1–4 (shaded fields linked by black arrows) from thermobarometric analysis (see text for discussion); alternative path traced by large dots also satisfies data base.

graywackes sometimes followed by climbing ripples, often ending with laminated layering in the upper shaly sequences. On the whole, the sequence may be interpreted as an association of mid-fan turbidites derived from a predominantly magmatic hinterland.

Deformation is weak with open, upright, large-wavelength folds ($\geq$ some 100 m) trending around 60°, no cleavage has been formed; weakly deformed quartz-veins – mostly subperpendicular to fold axes – and undeformed calcite-filled veins – paralleling the Rhine-graben, often with an oblique dip-slip lineation – crosscut the sequence (Fig. 3a). Shortening and compensating along-strike extension thus appear to characterize the orogenic mode of deformation of the sediments (comp. to granitoids, below).

Thin sections show evidence of weak crystal-plastic deformation and pressure solution of quartz, and fracturing of feldspars. The quartz texture (detrital grains as well as vein quartz) is largely recovered showing subgrains, discontinuous undulatory extinction, and incipient static recrystallization (Fig. 10b). The matrix is formed by newly grown biotite and muscovite (partly at the expense of plagioclase and quartz), both undeformed and lacking a preferred orientation (Fig. 10b). This assemblage may in some parts be retrogressed to quartz + sericite + kaolinite + hematite. Clearly, the weak deformation predates peak temperatures which are expressed in fabric recovery and postkinematic mica blastesis.

3.2.3. Metasediments at Weiler

In a number of quarries and minor outcrops near the village of Weiler (St. Germanshof) west of Wissembourg (4b in Fig. 1) a sequence (thickness > 100 m) – very similar to the Neustadt sediments – of graywacke-type metasediments, shales, and pyroclastic layers with an analoguous detrital composition is exposed (JUTEAU, 1971). The age is inferred to be ?Lower Carboniferous from a poorly preserved macrofauna (GENSER, 1965) and from the sediment type. Lithologic similarities with the nearby Val de Bruche sequence may also sugest an Upper Devonian age. Grain sizes and bed thicknesses of the greywackes are smaller compared to Neustadt (≤ 1 mm, ≤ 30 cm respectively), sole marks and channels are absent and – apart from laminations and cross bedding – internal sedimentary features are less conspicuous. The more pronounced matrix-supported grain fabric is suggestive of some mass flow transport of the turbidites (Fig. 10c).

Deformation is stronger than in the north with a steep dip of bedding (striking ca. 60°, Fig. 3c), numerous steep reverse faults (partly mineralised with Fe-poor chlorite), and a weak bedding-parallel pressure solution cleavage formed by the alignment of chlorite, sericite, biotite, and by elongated pressure-solved quartz grains (Fig. 10c, d). Apart from this aspect the deformational microfabrics and the related mineral assemblages are identical with the Neustadt/Hambach graywackes. The orogenic fabric is largely annealed (quartz) with peak biotite growth unoriented post-s_1 (Fig. 10d). Postorogenic brittle fractures contain dolomite or chlorite and show the same N-S-strike as undeformed lamprophyric dikes crosscutting the entire sequence; graywackes and lamprophyres are again unconformably overlain by Lower Permian clastics above a pronounced paleo-relief.

3.3. Granitoid intrusives

3.3.1. Petrography and kinematics

Granitoid magmatites occur in the Mid German Crystalline rise west of the river Rhine in the

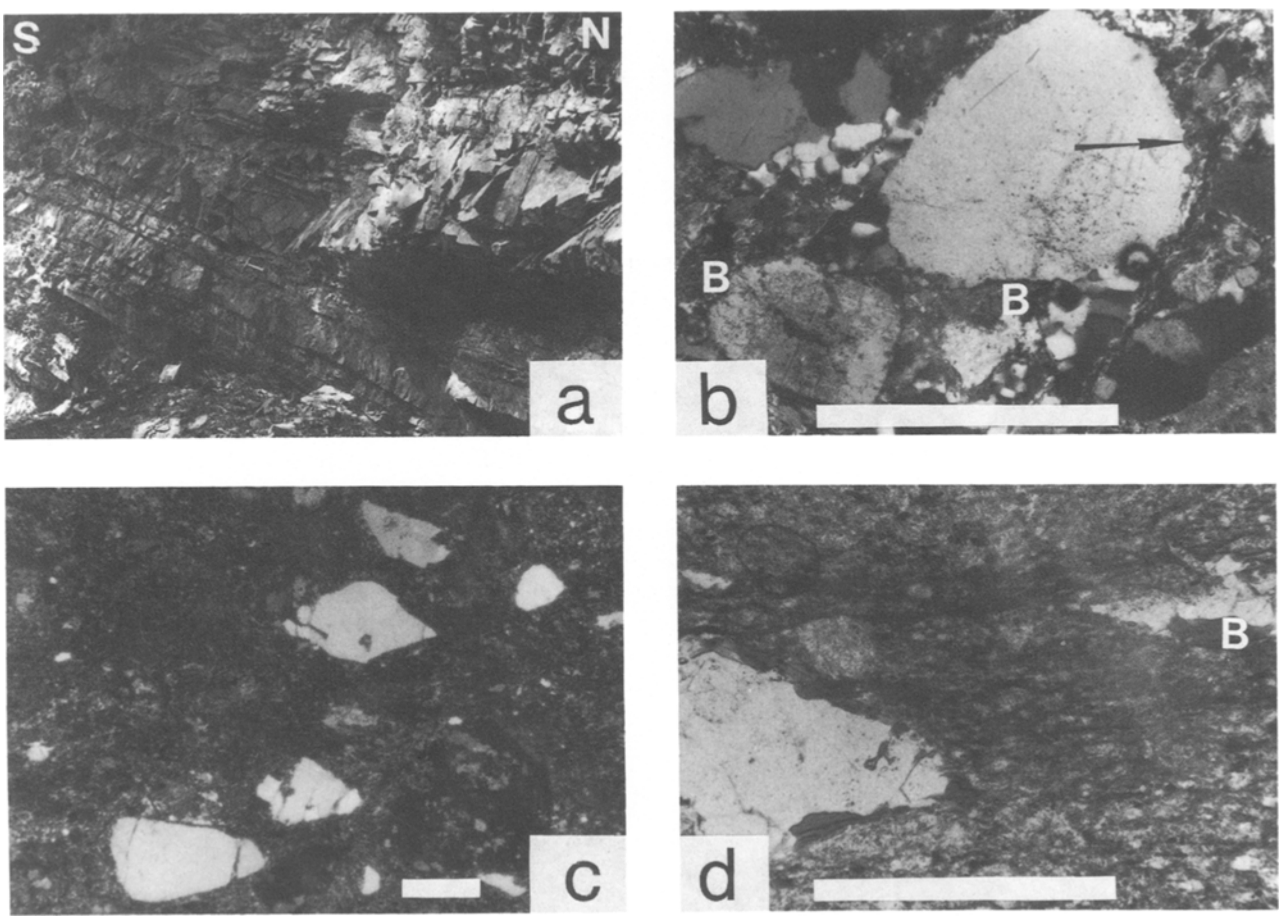

Fig. 10. Sedimentary features and fabric of graywackes at Hambach and Weiler/St. Germannshof; a) turbidite sequence at Hambach; b) subangular to rounded feldspars and some quartz (top right) in Hambach turbidites with equilibrated quartz grain boundaries and newly grown postkinematic biotite in matrix (B) and along embayed feldspar grain boundary (arrow); c) sedimentary texture of Weiler graywackes with magmatically corroded quartz and feldspar grains in matrix-supported fabric; d) early, boudinaged quartz veins subparallel to unconspicuous cleavage (subhorizontal) formed by aligned sericite/biotite, late- to postkinematic biotite (B) growing along rims of deformed quartz veins and replacing finegrained aligned matrix mica. b with crossed nicols; scale bar is 0.5 mm in all micrographs.

Schwarzbach-valley at Windstein west of Wissembourg (3c in Fig. 1), in the Kaiserbach-valley west of Landau (3b), and at Edenkoben in the northeast (3a; comp. ZAMINER, 1957). Geochemical investigations by LAUE et al. (1990) show the first two to be I-type granitoids and the Edenkoben granite to be crust-derived. MONTIGNY et al. (1983) have dated the Windstein granodiorite at 340 Ma (K-Ar on hbl + bio).

The Kaiserbachtal diorite consists of equigranular quartz, plagioclase + some green biotite, and minor K-feldspar (+ magnetite + epidote + zircon). All minerals have stable mutual grain boundaries. Weak solid state deformation is indicated by discontinuous undulatory extinction and by sutured grain boundaries of quartz, and by minor kinking of feldspars (Fig. 11c). The diorite contains conspicuous darker enclaves (Fig. 11a), which consist of plagioclase, biotite, quartz, and ?rhodonite in pink reaction rims (possibly resulting from decomposed garnet?) at the contact to the diorite. All minerals have straight grain boundaries. In the enclaves biotite also overgrows the idiomorphic plagioclase and anhedral quartz aggregates. The enclaves are elongated and define, along with shape-preferred oriented feldspars a crude magmatic foliation (Fig. 11a). On a larger scale this foliation is wrapped around amphibolite bodies (up to several tens of metres in size) contained in the diorite (Fig. 12a). The magmatic foliation defined by the intermediate and long axes of the mafic enclaves strikes at 60° (Figs. 3d, 12c). The enclave long and intermediate axes are horizontal and vertical respectively (Fig. 12c); the enclave shapes thus reflect an along strike stretching with plane-strain geometry (Fig. 12b) during magmatic emplacement.

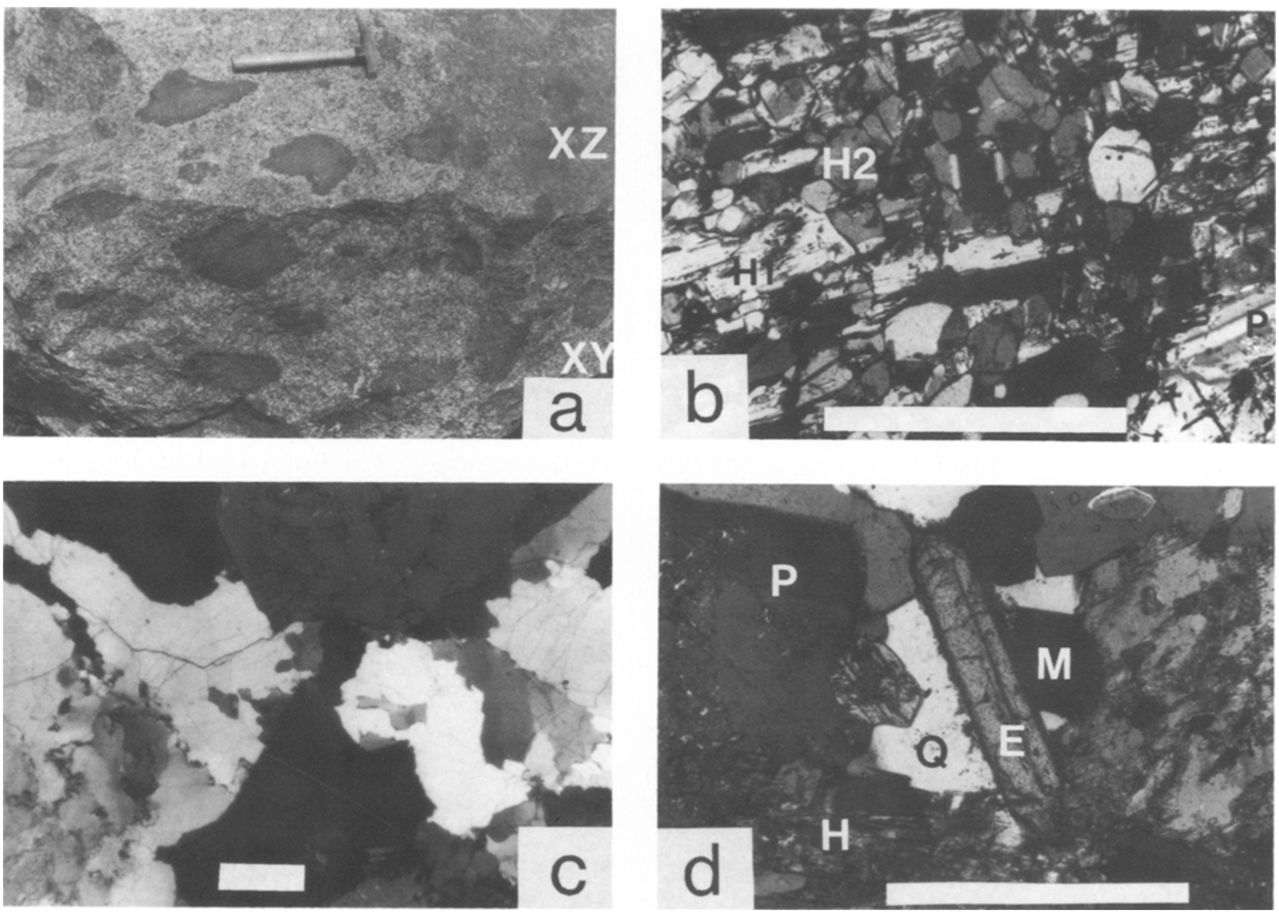

Fig. 11. Texture and petrography of Windstein and Kaiserbachtal granodiorites; a) weakly deformed and aligned xenoliths in Windstein granodiorite in two principal planes of strain (XY and XZ); b) texture in amphibolite body with early, partly altered and twinned hornblende (H1), plagioclase (P), and recrystallised unaltered postkinematic hornblende (H2); c) solid state deformation in Kaiserbachtal-granodiorite with undulous extinction, subgrain boundaries, and sutured grain boundaries in quartz; d) magmatic assemblage of hornblende (H), plagioclase (P), quartz (Q), magnetite (M), and Epidote (E) in Windstein-granodiorite. All micrographs with crossed nicolls, scale bar is 0.2 mm in all cases.

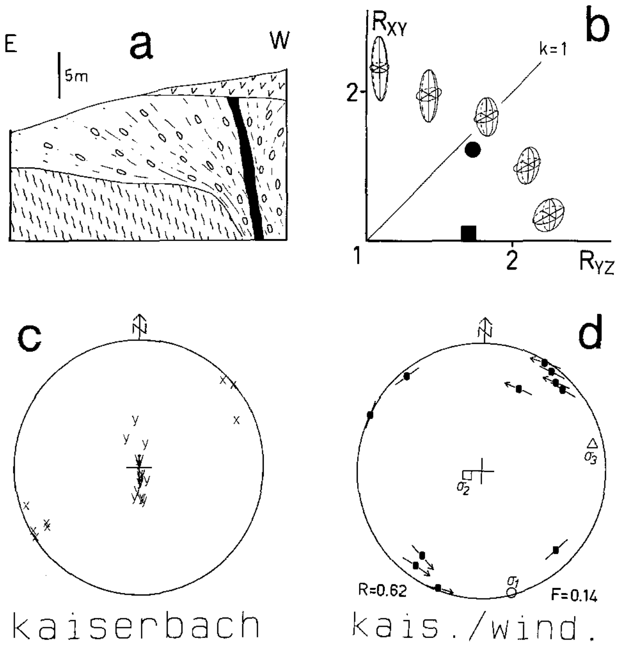

Fig. 12. Magmatic and postmagmatic fabric orientations in granitoids; a) schematic orientation of magmatic foliation (thin lines) and enclaves in northeastern quarry wall in the Kaiserbach-valley, lower striped sequence is large amphibolite body, black dike at right is late lamprophyric intrusion; b) strain or orientation geometry of xenolith shapes of the Kaiserbachtal-granodiorite (black circle) and of feldspar centre-to-centre distribution in Edenkoben-granite (black square) in Flinn-diagram; c) orientation of long (X) and intermediate (Y) xenolith axes in the granodiorite (comp. to poles of magmatic foliation in Fig. 3d = short xenolith axes) in lower hemisphere equal area projection; d) brittle faults from Kaiserbachtal- and Windstein-granodiorites with solution of stress-tensor calculation (comp. to Fig. 5b), for details of projection see Fig. 5.

The amphibolite xenoliths can be internally foliated (Fig. 3d). The foliation – discordantly cut at the magmatic contact – is marked by alignment of kinked and fractured hornblende with magnetite and undulatory plagioclase. Undeformed idioblastic hornblende grew during static recrystallization at the expense of the first generation (Fig. 11b). Plagioclase also recrystallized statically with a drop of An-content in the recrystallisate. Parts of the amphibolites are extensively altered and consist of layers of epidote and chloritized hornblende. Application of the hornblende-plagioclase geothermometer of SPEAR (1980) yields syn-foliation temperatures of 750–800 °C and ca. 600 °C during static annealing. The latter effect is possibly due to synintrusive heating of the large-scale amphibolite body which may be related to the 'Albersweiler' complex or a deeper rooted, previously deformed basement.

The Windstein granodiorite consists of up to 25% K-feldspar (+ plagioclase + quartz + biotite), some parts contain up to 10% of hornblende and associated accessory epidote (+ apatite + zircon + magnetite ± sphene + chlorite + muscovite, the last two replacing biotite + feldspar). Enclaves are again enriched in mafic minerals and show fabric orientations identical to the Kaiserbachtal outcrop. However, no amphibolite xenoliths were observed.

The Windstein granodiorite and the Kaiserbachtal diorite are deformed by a conjugate set of NW-SE and NE-SW oriented brittle faults, which contain subhorizontal slickenside lineations. Kinematic indicators show the same sense of slip displacement as in the gneiss basement at Albersweiler; plotting of all faults with their slickensides according to the method of HOEPPENER (1955) yields an identical kinematic pattern (comp. Figs. 12d and 5b). Calculation of the orientation of the paleostress-axes using the method of ETCHECOPAR et al. (1981, also see ONCKEN, 1988) gives the characteristic strike-slip orientation of stress axes with subhorizontal σ_1 and σ_3 in a NW-SE compressional regime with along-strike extension. This kinematic pattern is also reflected by the earlier magmatic fabric (comp. to enclave orientations in Fig. 12c). These observations suggest emplacement, cooling and concomittant brittle deformation during a persistent overall strike-slip kinematic regime.

Later NW-SE striking high angle normal faults show displacement towards the SW in the granodiorite. Carbonate occurs on cataclastic fractures. Postorogenic lamprophyric dikes in the Kaiserbachtal diorite strike N-S and are overlain along with the diorite by a Permian basaltic flow and coarse-grained continental clastics.

The Edenkoben granite contains roughly equal amounts of equigranular quartz, plagioclase and K-feldspar. Interstitial biotite makes up to ≤ 5 Vol.%. Muscovite + chlorite grew as secondary minerals at the expense of biotite and plagioclase. All minerals have straight or slightly lobate grain boundaries. The granite is intruded by granitic veins made up of roughly 60% K-feldspar (microperthite and microcline), 10% plagioclase and 30% quartz. Both, granite and the granitic veins have a weakly developed magmatic foliation, marked by an anastomosing alignment of biotite. The foliation forms a dome-like structure with a NW-SE trending axis (Fig. 3d) and flattening geometry Fig. 12b). Minor crystal plastic deformation is indicated by local feldspar undulation and by additional subgrain formation and incipient recrystallization in quartz. Weak cataclastic deformation is confined to subvertical NE-SW striking, discrete extensional fractures filled by quartz and sericite. The Edenkoben granite is devoid of strike slip faults.

3.3.2. Barometry of the intrusives

Constraints on the intrusion depths of the granitic rocks were obtained using the Si-content per formula unit of the phengite component in muscovite (MASSONNE & SCHREYER, 1987) and the total Al per formula unit contained in calcic hornblende within a defined limiting assemblage of Qz + Plag + Kspar + Bio + Hbl + Mt + Sph ± Ep (Al_T-method of HAMMARSTROM & ZEN, 1986).

In the undeformed Edenkoben granite the Si content in the muscovite is on average 3.14. Muscovite + chlorite grew as secondary minerals at the expense of biotite. The reaction temperature cannot be calculated exactly, it was, however, taken to be below the solidus granodiorite temperature and, probably, below biotite stability. The maximum value obtained thus gives an intrusion depth of 1.5 kb (at 300 °C) and of 3 kb (at 550 °C). The data thus correspond to a cooling depth of 4−8 km which is near the original intrusion depth probably.

The average Al_T-content in hornblendes of the Windstein granodiorite is 1.33, suggesting an intrusion depth of 2.5 kb equivalent to about 7 km. The maximum intrusion depth (Al_T: 1.4) is around 9 km, whereas the minimum intrusion depth recorded is around 4 km (Al_T: 1.1). This corresponds well with the range of intrusion depths obtained by phengite barometry in the Edenkoben granite. Obviously thus, all solid state deformation of the granitoids is acquired during cooling at upper crustal levels, mostly in the brittle field below the plastic yield strength.

4. Discussion

4.1 The orogenic state of the crust

Essential for the characterization of the physical state of the Saxothuringian crust west of the river Rhine during its orogenic evolution are the features listed below:

- The Upper Devonian and Lower Carboniferous graywackes are largely dominated by magmatic detritus; a weak polarity is hinted at by a general grain size refinement from south (northern Vosges; comp. WICKERT & EISBACHER, 1988) to north (Saar 1 well; comp. HERING & ZIMMERLE, 1976); a concomittant increase in the share of carbonates in the Upper Devonian sequence + a decrease of pyroclastic layers (comp. Fig. 14) can be observed.
- A primarily hot crust is indicated by active volcanism during Upper Devonian/Lower Carboniferous times including the possible formation of contact metamorphic aureoles (Burrweiler).
- Synorogenic metamorphism as well as deformation decrease towards the north resulting in an oblique internal deformation front within the Saxothuringian zone during the post-Mid-Devonian orogenic pulse; moreover, syn- to late-orogenic PT-conditions indicate LP-HT metamorphism in a crust with a strongly disturbed geotherm in the final stage (average grad. T > 60°/km).
- The Albersweiler orthogneiss-complex shows an early stage of isothermal decompression with coaxial deformation which both are not observed in the other units.
- Deformation − during ?Late Devonian and Early Carboniferous − is weak with formation of only one pervasive fabric at most and is not generally accompanied by major crustal stacking and thickening of the upper crust − with exception of the medium-P Burrweiler unit.
- Shallow intrusion depths of plutonic rocks and restricted deformation around 340 Ma during retrogressive uplift suggest only limited unroofing; the overall associated shortening direction affecting all units was NW-SE with concomittant orogen-parallel stretching (strike-slip kinematics) − starting apparently during the synorogenic magmatic phase at the latest.

Essentially, the crystalline rise west of the river Rhine represents a crustal segment which is dominated by thermal rather than tectonic processes during probably a single orogenic imprint (comp. PT-paths in Fig. 13). All, generally weakly deformed sedimentary rocks exhibit postkinematic heating, in cases even include possible indications of prekinematic heating (Burrweiler). The presence of abundant magmatic associations of different ages relative to deformation agrees well with this observation. On the whole, the rock association can easily be explained to form a coherent crustal unit. The geologic relationships do not evoke major reverse- or wrench faulting to reconcile the juxtaposition of different rock units. Even the abnormal PT-evolution of the Burrweiler sediments can be explained by a prekinematic contact metamorphic environment prior to synkinematic pressure increase. The latter can possibly be related to minor crustal stacking (?overthrust by the Albersweiler complex from the south). The relative timing to peak metamorphic conditions and the pervasive deformation of the Albersweiler complex relate to an either Early Variscan (Lower Devonian) deformation or to the Cadomian orogenic period. The latter possibility is hinted at by the findings of Cadomian (ca. 540 Ma)

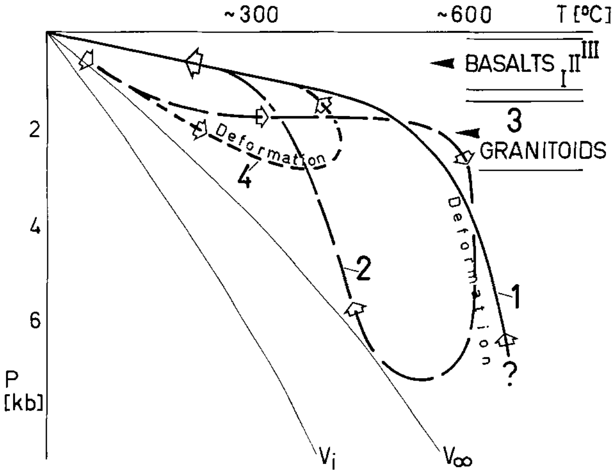

Fig. 13. Synoptical P-T-D paths of Variscan rock sequences of western Rhine-graben escarpment; numbers are identical to numbers in Fig. 1; 1: Albersweiler gneiss; 2: Burrweiler schists; 3: granitoids; 4: Neustadt/Hambach and Weiler graywackes; V_i shows initial stable geotherm in continental crust, V_{oo} shows equilibrated geotherm after stacking of continental crust calculated by ENGLAND & THOMPSON (1984); the relative timing of pervasive deformation and of intrusive activities during thermal evolution are indicated.

magmatic (calc-alcaline) cobbles in flysch of the Rhenohercynian zone to the north (SOMMERMANN, 1990) and by a similar age found by M. SCHWAB et al. (pers. comm.) for a diorite drilled in the eastern Mid-German Crystalline Rise.

The extremely incomplete exposure of this part of the Saxothuringian clearly does not allow the detailed reconstruction of a geodynamic scenario. However, the major aspects established, together with available geochemical, geophysical, and sedimentological data imply a set of minimum constraints which must be met by any model proposed.

4.2. Geodynamic setting

The earliest evolutionary stage, recorded in the Albersweiler basement, is only vaguely outlined. The present data on the combined metamorphic and structural evolution (decompression and coaxial stretching, see above) can be seen as related to exhumation either due to a stage of stretching in a crustal thinning régime or to a stage of crustal stacking and erosion. The age of this stage is poorly constrained at present (see above mentioned possibilities).

Comparison of the sedimentary sequences described in the present paper with those drilled in the Saar 1 well or exposed in the northern Vosges clearly shows that a, possibly fragmentary, carbonate platform had developed during Mid-Devonian times on an obviously then still stable continental platform (crystalline, Saar 1 well, or Lower Paleozoic sedimentary basement, northern Vosges). This sequence is overlain by an Upper Devonian to Lower Carboniferous volcano-sedimentary sequence with predominantly magmatic detrital material assembled in graywackes, turbidites, and shales. Obviously, the Saxothuringian crust west of the Rhine went through an important change at the mentioned time boundary, the stable platform disintegrated by (calcalcaline!) magmatic and, later-on, also deformational processes (see below; Fig. 14). The orogenic imprint is clearly governed by a thermal event with a peak during the Lower Carboniferous overall strike-slip regime. Moreover, the onset of orogen-parallel extension compensating for crustal shortening seems to be related to the timing of closure of the minor ?oceanic basin (e.g. ENGEL & FRANKE, 1983; ENGEL et al., 1983) intervening between the Saxothuringian zone and the Rhenohercynian passive margin. Collision and overthrusting of the latter by the Saxothuringian thus marks a change of deformation mode in the southern crustal unit. The post peak-deformational geothermal state at about 340 Ma led to fabric equilibration and indicates a substantially disturbed geotherm (comp. Fig. 13). The latter aspect can not be explained by the consequence of crustal stacking and thickening during continental collision with subsequent thermal reequilibration – the stable geotherms calculated by ENGLAND & THOMPSON (1984) for that case are definitively too low (see. Fig. 13). Rather, the thermal state of the crust has to be related to major magmatic advective heat input into the crust and possibly to some, if at all, late crustal extension. Late-orogenic calcalcaline lamprophyres (~ 330 Ma) sealed the contractional faults and intruded into a largely cooled and eroded crust (comp. model in Fig. 15).

Although no single observation yields unequivocal evidence, the outlined thermal state, the tectonometamorphic evolution during orogenic contraction, and the type of magmatites and sediments involved together provide some of the key elements for the assessment of the possible geodynamic setting. Incorporating the findings on the nearby Odenwald mountains by KROHE (1991) and WILLNER et al. (1991) and the common juxtaposition against the High-P Phyllite Zone at the southern rim of the Rhenohercynian further narrows down possible interpretation (also see occurance of magmatites with MOR-affinity, see introduction).

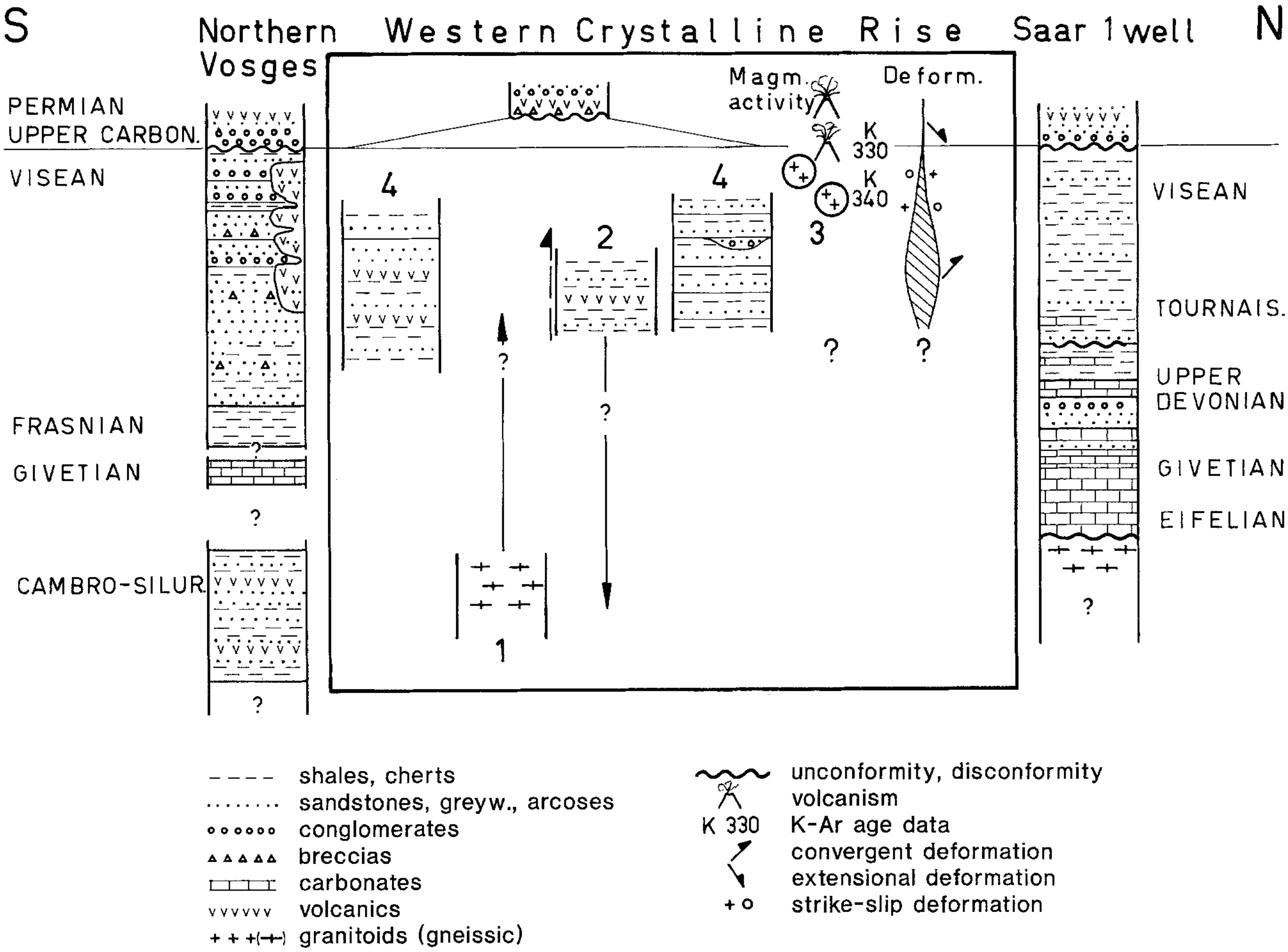

Fig. 14. Time-space chart of western Saxothuringian microplate in a N-S section; data on Northern Vosges from WICKERT & EISBACHER (1988), on Saar 1 well from HERING & ZIMMERLE (1976), in Western Crystalline Rise from data cited and established in the present paper. Figures 1–4 refer to lithologic groups indicated in Fig. 1. Due to tectonic contacts or preservation only in olisthostrome boulders (Mid-Devonian) the northern Vosges sequence does not necessarily reflect a coherent section.

An intra-magmatic-arc setting on continental crust evolving prior to and during the Lower Carboniferous collision of the Saxothuringian microplate with the Rhenohercynian passive continental margin appears to be the most probable inference. The sedimentary record west of the Rhine further suggests a partly submarine intra- or forearc depositional setting evolving during Late Devonian times on stretched continental crust and persisting during continental collision until the Late Lower Carboniferous. Within the Variscan framework this – rather small volume arc – only marks a minor feature related to the closure of a minor basin. This inferred evolutionary pattern is superposed on the large-scale plate-kinematic pattern of the Gondwana-Laurasia collision at the southern margin of the Variscan microplate collage transforming the internal (Moldanubian) parts into a major magmatic arc as discussed by e.g. LEEDER, 1982; LORENZ & NICHOLLS (1984), ZIEGLER (1986), MATTE (1986), FINGER & STEYRER (1990).

The proposed magmatic arc setting is also supported by recent geochemical analyses of all intrusives from the Northern Vosges to the Edenkoben area which show two groups of intrusives (see LAUE et al., 1990; WILDBERG, 1990). The granodiorites and diorites from the Northern Vosges, Windstein, Kaiserbach, and the basaltic intrusives at Albersweiler all show a clear subduction-related I-type fingerprint. The younger, late- to postkinematic Edenkarbon granite further north and the nearby Burrweiler micrograntes on the other hand have an S-type signature. Possibly this magmatic sequence indicates a change from an arc environment evolving through crustal thickening by underplating of the Rhenohercynian ocean to the post-collisional state of a thickened, intruded, and overheated crust which spreads under partial melting.

This supposed evolution, apart from preserving the sedimentary cover, differs considerably from that shown east of the river Rhine. Crustal thickening, uplift, and erosion do not seem to take a significant part in the west while increasingly deeper-rooted basement with barrovian metamorphism (Spessart) is exhumed to the northeast in several steps. The latter are marked by major, steep, N-S trending faults showing sinistral strike slip motion and oblique extension (comp. WICKERT & EISBACHER, 1988; KROHE, 1991; WEBER, 1990; WICKERT et al., 1990; also comp. similar faults at Albersweiler). On the other hand, the structural and magmatic evolution of the southern Odenwald – although exposed more deeply – is very similar to that met on the opposite Rhine graben flank (comp. KROHE, 1991; HENNES-KLAIBER, 1990).

4.3. Concluding remarks

The geomagnetic pattern of the Saxothuringian zone shows major subelliptical anomalies with upper crustal sources (intermediate to basic magmatites and magnetised metasediments; WONIK & HAHN, 1989; EDEL & FLUCK, 1989). Contrastingly the adjacent Rhenohercynian and the Moldanubian zones are magnetically quiet. The strike of the Saxothuringian magnetic zone is oriented somewhat obliquely to the Variscan zone boundaries: SW-NE as opposed to the general ENE-WSW strike of the zone boundaries (Fig. 16). It clearly coincides with the drilled and outcropping occurances of magmatic rocks, the remaining areas being dominated by low grade to unmetamorphic Paleozoic sediments. The traditionally inferred continuation of the Mid-German

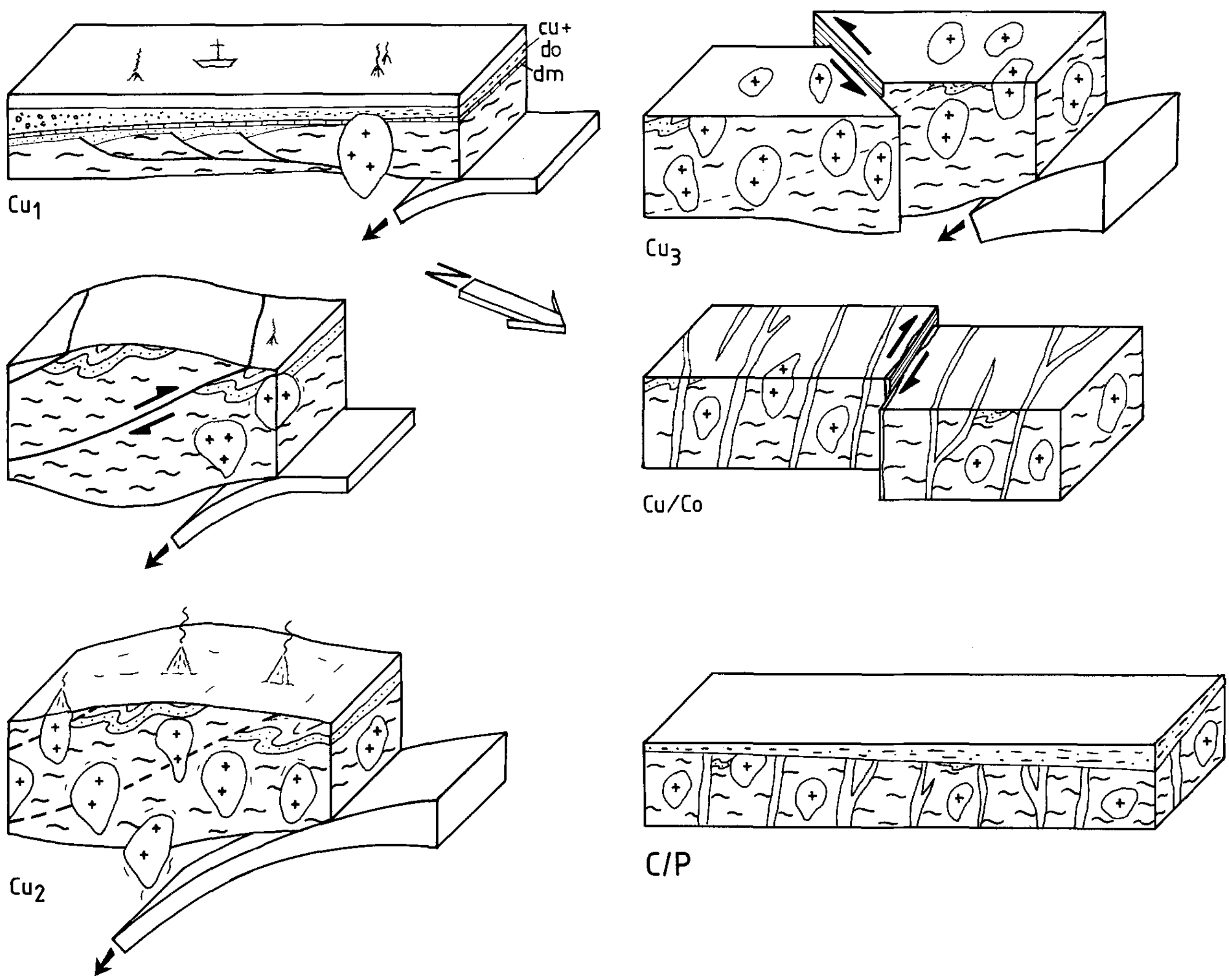

Fig. 15. Schematic interpretative sequence of evolutionary steps in the geodynamic development of Western Crystalline Rise based on minimum requirements established by the present study (see text for details); thickening of lower plate suggests onset of continental collision.

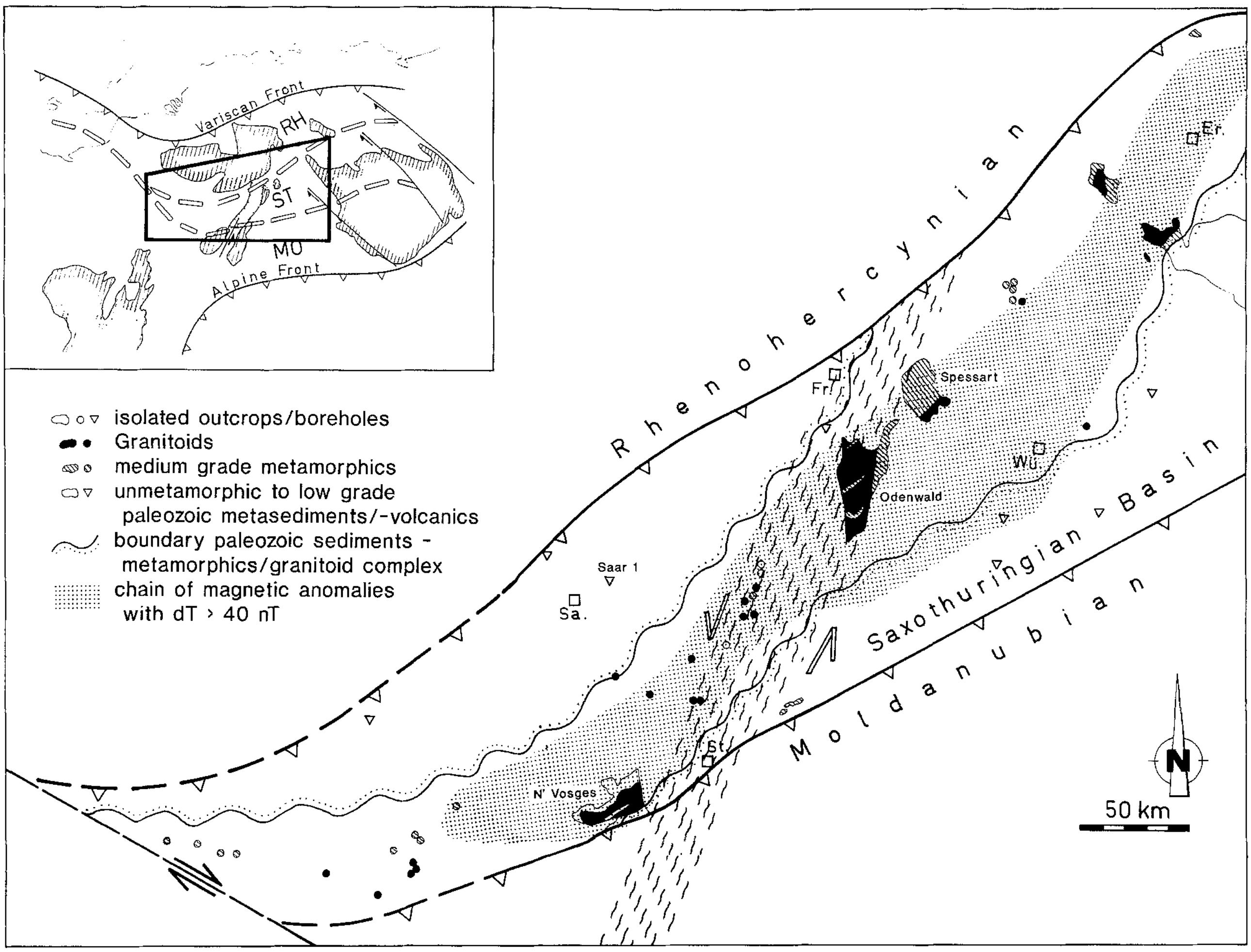

Fig. 16. Schematic map of Saxothuringian microplate from the inferred Bray fault in the west (see HOLDER & LEVERIDGE, 1986) to the Thuringian forest in the east showing extent and position of the basins (large wavy lines), outcrops of metamorphic Variscan basement and occurrence of synorogenic granitoids, area of peak magnetic anomalies with $T > 40$ nT (shaded; from WONIK & HAHN, 1989, and EDEL & FLUCK, 1989), and location of late-orogenic sinistral wrench-fault system (short wavy lines). Northwestern part of the basin contains undeformed and unmetamorphic Mid-Devonian to Lower Carboniferous sediments, the southeastern basin has a deformed Paleozoic filling. Pre-Upper Carboniferous basement lithologies in boreholes are compiled from HERING & ZIMMERLE (1976), DONSIMONI (1981), and KÄMPFE (1984). Indicated zone boundaries are largely characterized by not specified oblique dextral slip (see ONCKEN, 1988; WICKERT & EISBACHER, 1989; WICKERT et al., 1990).

Crystalline Rise towards the west (BRINKMANN, 1948) is thus interpreted differently in this paper. Its northwestern border furthermore roughly marks a deformation front within the Saxothuringian – the Eifelian to Visean basin filling drilled by the Saar 1 well is undeformed on a regional scale as supported also from recent seismic data (e.g. DEKORP RESEARCH GROUP, 1991, see also DONSIMONI, 1981). Through the Upper Devonian/Lower Carboniferous the above area apparently occupies the position of a forearc basin riding piggy-back on the edge of the evolving active margin.

The Devono-Carboniferous sedimentary sequences west of the river Rhine (see Fig. 14) moreover differ considerably from the basin filling of the Saxothuringian proper – the latter is characterised by abundant basaltic volcanics at the period mentioned. This basin is interpreted by FRANKE (1989) to have formed by rifting in Lower Paleozoic times, possibly in a back arc setting as inferred by ZIEGLER (1986), on continental crust and is superseded by a subsequent Lower Carboniferous accretionary environment upon approach of the Moldanubian cordillera. The incipient magmatic arc sensu strictu building up on the former stretched continental crust with its axis reaching from the Northern Vosges in the SW to the Thuringian Forest in the NE would thus separate the western Saxothuringian from the Saxothuringian basin proper from Upper Devonian times onwards. The entire Saxothuringian microplate may possibly have obtained this internally oblique polarity during oblique subduction and docking at the passive margin of the Rhenohercynian zone. The latter shows abundant evidence of dextral shearing during late stage deformation (ONCKEN, 1988; ANDERLE et al., 1990) following peak metamorphism at ca. 325 Ma (AHRENDT et al., 1983). During the Lower Carboniferous, furthermore, the above mentioned kinematics – dextral at Rhenohercynian-Saxothuringian boundary, sinistral intra-Saxothuringian (this paper and KROHE, 1991) – result in a westward expulsion of the intervening wedge of the West-Saxothuringian basin. Its final stage, respectively the initial evolution of the Permo-Carboniferous Saar-Nahe successor basin thus seems to relate to a continental escape situation in its broadest sense.

Alternatively WEBER (1990) proposed that the Rhinegraben parallel wrench fault system represents an intra-Saxothuringian transform fault. This system is taken to account for the evolution of the Saar-Nahe basin as a pull-apart basin, for the abundance of synorogenic intrusives ('leaky transform'), and for the juxtaposition of Barrovian type metamorphic basement in the east against the LP/HT-rocks west of the fault. However, timing constraints for sinistral wrench faulting on Rhine-graben parallel faults place the lower limit at post-peak metamorphism (see earliest K-Ar cooling ages on hbl around 370 Ma in the Odenwald area by KREUZER & HARRE, 1975, and related kinematics by KROHE, 1991), the upper limit being given by crosscutting undeformed lamprophyric dikes dated around 330 Ma (FRENZEL, 1971; HESS & SCHMIDT, 1989). Sedimentation in the Saar Nahe basin, on the other hand, starts already in Mid-Devonian times and lasts – interrupted by several hiatuses – until the Lower Permian (SCHÄFER, 1989). Furthermore the Lower Carboniferous sedimentary record is not indicative of a pull apart setting.

The major, if little understood role of the N-S trending Rhine-graben parallel wrench faults in the crustal evolution of the western Mid German Crystalline Rise is not questioned however. Rather, their importance for juxtaposing basement deeply eroded during Lower Carboniferous times against barely exhumed sequences with contemporaneous sedimentation must be underlined. A submerged western end of a magmatic arc – as opposed to the eastern continuation – subjected to syn- and late-orogenic wrench-faulting might be able to meet the above requirements. Moreover, it appears that the switch to strike-slip deformation is related to the phase of continental collision at the Rhenohercynian-Saxothuringian boundary which is dated by the first arrival of flysch in the Rhenohercynian basin following closure of the intervening oceanic basin (e.g. ENGEL & FRANKE, 1983; FLOYD et al., 1990). Apparently, the mode of large scale crustal deformation in the upper plate upon collision is changed during concomittant crustal imbrication.

Acknowledgements

Without the assistance of H. Johanning and R. Elsner with diffractometric and SEM analysis much of the above results would never have been achieved. R. Schaeffer (Basalt-Actien Gesellschaft) kindly allowed field work in the Albersweiler quarry during several occasions. G. Kowalczyk, S. Laue, Th. Reischmann, K. Emmermann, and G. Kobberger have helped clearing our ideas by fruitful discussion during common field trips. The criticisms of G. Kowalczyk, M. Okrusch, E. Stein and an anonymous reviewer on an earlier draft has greatly improved the logic of our arguments. All help by the named is gratefully acknowledged.

Appendix

The thermobarometric analyses were carried out using a wave-length dispersive spectrometer on a Cambridge SEM type S4. Analyses were obtained with a standard setup of 20 kV acceleration voltage, a tilt angle of 20°, and a take-off angle of 45,7° with a beam diameter of $< 5\ \mu m$. Standards used included hornblende (kindly provided by G. Brey, Mainz), biotite, garnet, and plagioclase. The raw data were corrected by a ZAF calculation.

Calculation of formula units for each analysed mineral was done by a software package supplied by H. M. BRAUN (unpublished) based on numerical iterative partitioning of the involved elements. The estimated error with the equipment and the procedure applied generally is below 10% relative/element which as a rule is well below the error margin usually assigned to thermobarometric calibrations ($\pm$ 50 °C, $\pm$ 1 kb) derived by empirical as well as by thermodynamic data sets. Si-content in phengites which were measured without standards in most cases are 5–10% relative higher than the true values resulting in somewhat exaggerated calculated pressures.

The thermobarometric study was aimed at establishing the gross P/T-ranges of metamorphism (e.g. HT versus LT; HP versus LP) in order to reveal general trends during the metamorphic evolution. The P/T data are thus not to be taken as exact as suggested by the numbers given in the following tables (table 1–3).

Table 1. Albersweiler.

rock:	hornblende-gneiss		amphibolite				basalt II	
mineral:	hbl	plag	hblI	hblII	plagI	plagII	hblI	hblII
N	2	6	2	2	2	1	2	2
Na_2O	0.89	6.59	0.98	0.18	7.78	7.82	0.41	0.90
sigma	0.14	0.62	0.08	0.09	0.16	-	0.04	0.2
MgO	12.78		15.61	18.51			17.72	14.44
sigma	0.14		0.03	0.08			0.49	2.79
Al_2O_3	10.34	24.95	9.39	2.9	26.3	26.29	4.44	7.84
sigma	0.38	2.06	0.02	0.22	1.03	-	0.17	3.17
SiO_2	48.52	63.56	48.39	56.69	62.3	63.16	53.39	47.95
sigma	0.15	3.05	0.9	0.58	1.86	-	0.95	3.74
K_2O	0.89	0.3	0.67	0.06	0.35	0.62	0.05	0.11
sigma	0.07	0.28	0.04	0.02	0.28	-	0.05	0.08
CaO	11.73	4.6	12.87	13.16	4.44	3.51	11.35	8.06
sigma	0.05	0.57	0.31	0.11	0.16	-	0.43	2.14
TiO_2	0.55		0.56				0.19	0.92
sigma	0.03		0.13				0.17	0.59
CrO_2	0.05							
sigma	0.01							
MnO	0.37							
sigma	0.02							
FeO	13.86		10.3	8.6			11.53	17.19
sigma	0		0.52	0.2			0.09	0.11
Mol% An		27			24	19		
Al_T p.f.u.	1.67		1.57	0.47			0.72	0.79
P-T	**540°C/4kb[3]**		**I: 530°C/3.5kb[3]; II: 520°C/ 2kb[3]**				**< 1kb[2]**	

Table 2. Intrusives.

rock:	garnet-biotite schist					cordierite-biotite schist
mineral:	garnet centre	garnet outer core	garnet rim	bio	pheng	pheng
N	4	3	4	6	2	4
MgO	2.53	2.66	2.58	4.79	2.75	3.28
sigma	0.27	0.03	0.17	0.4	0.96	0.03
Al_2O_3	22.57	22.41	22.66	25.11	31.97	30.87
sigma	0.21	0.05	0.13	1.5	1.9	0.23
SiO_2	39.03	38.86	39.06	46.34	49.88	53.84
sigma	0.22	0.15	0.12	0.98	0.9	0.89
K_2O				8.35	8.68	9.63
sigma				0.75	0.15	0.56
CaO	0.73	0.78	0.74			
sigma	0.05	0.06	0.03			
TiO_2				1.24	1.26	0.16
sigma				0.24	0.59	0.16
MnO	2.51	2.44	2.46			
sigma	0.16	0.02	0.1			
FeO	32.63	32.84	32.52	14.17	5.5	2.21
sigma	0.17	0.1	0.11	1.63	2.61	0.38
Mol% Alm	80.3	79.9	80.2			
Pyr	11.1	11.6	11.3			
Spess	6.3	6	6.2			
Gross	2.3	2.5	2.3			
Fe/(Fe+Mg)	0.875	0.87	0.875			
Si p.f.u.					3.15 - 3.2	3.2 - 3.3
P-T	**550°C[5,6](6-8kb)**				**2 kb[4](300°C)**	**6-8 kb[4](550°)**

Calculated PT-data according to thermo-barometers from:
[1] Spear (1980); [2] Hammarstrom & Zen (1986); [3] Plyusnina (1982);
[4] Massonne & Schreyer (1987); [5] Ferry & Spear (1978); [6] Spear & Cheney (1989)

locality/ rock:	Kaiserbachtal- amphibolite-xenolith				Windstein- granodiorite	Edenkoben- granite
mineral:	hblI	hblII	plagI	plagII	hbl	pheng
N	2	3	3	2	3	6
Na_2O	1.05	1.11	3.62	5.73	0.78	0.06
sigma	0.44	0.14	0.57	0.34	0.06	0.05
MgO	13.56	13.24			15.23	1.39
sigma	0.4	0.76			0.28	0.22
Al_2O_3	7.3	7.3	31.79	28.54	4.25	35.5
sigma	1.02	0.42	0.25	0.91	0.31	0.65
SiO_2	50.29	49.03	54.4	58.56	49.57	48.83
sigma	2.14	1.08	2.12	0.77	0.92	0.32
K_2O	0.24	0.24	0.06	0.19	0.27	11.31
sigma	0.14	0.06	0.05	0.06	0.05	0.1
CaO	11.64	11.58	11.25	7.1	11.85	
sigma	0.07	0.13	1.29	0.82	0.1	
TiO_2	0.92	0.83			0.27	0.72
sigma	0.31	0.24			0.11	0.24
MnO	0.14					
sigma	0.14					
FeO	14.94	16.43			12.5	2.19
sigma	0.78	0.46			0.14	0.23
Mol% An			62	40		
Al_T p.f.u.					1.33	
Si p.f.u.						3.14
P-T	I: 750-800°C[1]; II: 600°C[1]				2.5 kb[2]	1.5kb(300°)-3kb(550°)[4]

Table 3. Burrweiler.

References

AHRENDT, H., CLAUER, N., HUNZIKER, J. C. & WEBER, K. (1983): Migration of Folding and Metamorphism in the Rheinisches Schiefergebirge Deduced from K-Ar and Rb-Sr Age Determinations. – In: Intracontinental Fold Belts. Case Studies in the Variscan Belt of Europe and the Damara Belt in Namibia (eds.: H. Martin and F. W. Eder). Springer, Berlin Heidelberg New York Tokyo, pp. 323–338.

ANDERLE, H. J., MASSONNE, H. J., MEISL, S., ONCKEN, O. & WEBER, K. (1990): Southern Taunus Mountains. – In: Conf. Paleozoic Orogens in Central Europe, Field Guide Mid German Crystalline Rise & Rheinisches Schiefergebirge, 125–148.

BEHRMANN, J., DROZDZEWSKI, G., HEINRICHS, T., HUCH, M., MEYER, W. & ONCKEN, O. (1991): Crustal-scale balanced cross sections for parts of the central EGT-segment. – Tectonophysics, **196**, 1–21.

BRINKMANN, R. (1948): Die Mitteldeutsche Schwelle. – Geol. Rdsch. 56–66.

DEKORP Research Group (1991): Results of the DEKORP 1 (BELCORP-DEKORP) deep seismic reflection studies in the western part of the Rhenish Massif. – Geophys. J. Int., **106**, 203–227.

DONSIMONI, M. (1981): Le Bassin Houiller Lorrain. – Mèm. Bur. Rech. Géol. Min., **117**, 102 pp., 15 planches Orléans CEDEX.

EDEL, J. B. & FLUCK, P. (1989): The upper Rhenish Shield basement (Vosges, Upper Rhinegraben, and Schwarzwald): Main structural features deduced from magnetic, gravimetric, and geological data. – Tectonophysics, **169**, 303–316.

ENGEL, W. & FRANKE, W. (1983): Flysch-Sedimentation: Its Relations to Tectonism in the European Variscides. – In: H. Martin and F. W. Eder (Editors), Intracontinental Fold Belts. Case Studies in the Variscan Belt of Europe and the Damara Belt in Namibia. Springer, Berlin Heidelberg New York Tokyo, pp. 289–321.

—, —, GROTE, C., WEBER, K., AHRENDT, H. & EDER, F. W. (1983): Nappe Tectonics in the Southeastern Part of the Rheinisches Schiefergebirge. – In: H. Martin and F. W. Eder (Editors), Intracontinental Fold Belts. Case Studies in the Variscan Belt of Europe and the Damara Belt in Namibia. Springer, Berlin Heidelberg New York Tokyo, pp. 267–287.

ENGLAND, P. C. & THOMPSON, A. (1984): Pressure-Temperature-Time Paths of Regional Metamorphism I. Heat Transfer during the Evolution of Thickened Continental Crust. – J. Petrol., **125**, 894–928.

ETCHECOPAR, A., VASSEUR, G. & DAIGNIERES, M. (1981): An inverse problem in microtectonics for the determination of stress tensors from fault striation analysis. – J. Struct. Geol., **3**, 51–65.

FERRY, J. M. & SPEAR, F. S. (1978): Experimental Calibration of the Partitioning of Fe and Mg Between Biotite and Garnet. – Contrib. Mineral. Petrol., **66,** 113–117.

FLOYD, P. A. (1984): Geochemical characteristics and comparison of the basic rocks of the Lizard Complex and the basaltic lavas within the Rhenohercynian troughs of SW England. – J. geol. Soc. London, **141,** 61–70.

—, LEVERIDGE, B. E., FRANKE, W., SHAIL, R. & DÖRR, W. (1990): Provenance and depositional environment of Rhenohercynian synorogenic greywackes from the Giessen Nappe, Germany. – Geol. Rdsch., **79,** 611–626.

FRANKE, W. (1989): Tectonostratigraphic units in the Variscan belt of Central Europe. – Geol. Soc. Amer. Spec. Pap., **230,** 67–90.

— & ONCKEN, O. (1990): Geodynamic evolution of the North-Central Variscides – a comic strip. – In: The European Geotraverse: Integrative Studies (eds.: R. Freeman, P. Giese, and St. Mueller), Results from the 5th Study Centre 26. 3. – 7. 4. 1990, pp. 187–194, European Science Foundation.

FRENZEL, G. (1971): Die Mineralparagenese der Albersweiler Lamprophyre (Südpfalz). – N. Jb. Miner. Abh., **115,** 164–191.

GENSER, H. (1965): Fossilfunde aus den Schiefern von Weiler bei Weißenburg/Elsaß. – Jber. u. Mitt. oberrh. geol. Ver., N.F., **47,** 153–157.

GRÖSSER, J. & DÖRR, W. (1986): MOR-Typ-Basalte im östlichen Rheinischen Schiefergebirge. – N. Jb. Geol. Paläont. Mh., **12,** 705–712.

HAMMARSTROM, J. M. & ZEN, E. (1986): Aluminium in hornblende: An empirical igneous geobarometer. – Amer. Mineral., **71,** 1297–1313.

HÄNTZSCHEL, W. (1972): Lebensspuren in den Kulm-Tonschiefern von Neustadt a.d. Weinstraße. – Oberrhein. Geol. Abh., **21,** 107–115.

HENES-KLAIBER, U. (1989): Der Odenwald: Hinweise auf einen variszischen Arc-Magmatismus? – Beih. z. Europ. J. Mineral., **1/1,** 66.

HERING, O. & ZIMMERLE, W. (1976): Petrographische Beschreibung und Deutung der erbohrten Schichten (Saar 1). – Geol. Jb., **A27,** 91–306.

HESS, J. C. & SCHMIDT, G. (1989): Zur Altersstellung der Kataklasite im Bereich der Otzberg-Zone, Odenwald. – Geol. Jb. Hessen, **117,** 69–77.

HOEPPENER, R. (1955): Tektonik im Schiefergebirge. – Geol. Rdsch., **44,** 26–58.

HOLDER, M. T. & LEVERIDGE, B. E. (1986): Correlation of the Rhenohercynian Variscides. – J. geol. Soc. London, **143,** 141–147.

ILLIES, H. (1963): Der Westrand des Rheingrabens zwischen Edenkoben (Pfalz) und Niederbronn (Elsaß). – Oberrhein. Geol. Abh., **12/3,** 1–24.

JUTEAU, T. (1971): Nouvelles données cartographiques, pétrographiques et chimiques sur le massif dévono-dinantien du Rabodeau (Vosges septentrionales) – Pétrogenèse d'une série spilite-Kératophyre 'hercynotype' complexe. – Sci. de la Terre, **16/1,** 45–106, Nancy.

KÄMPFE, C. (1984): Tiefbohrungen in Baden-Württemberg und umgebenden Ländern. – Arb. Inst. Geol. Paläont. Univ. Stuttgart, N. F., **80,** 313 pp., Stuttgart.

KIRSCH, H., KOBER, B. & LIPPOLT, H. J. (1988): Age of intrusion and rapid cooling of the Frankenstein gabbro (Odenwald, SW Germany) evidenced by $^{40}Ar/^{39}Ar$ and single zircon $^{207}Pb/^{206}PB$ measurements. – Geol. Rdsch., **77,** 693–711.

KREUTZER, H. & HARRE, W. (1975): K/Ar-Altersbestimmungen an Hornblenden und Biotiten des Kristallinen Odenwaldes. – Aufschluß 27 (Sonderband Odenwald) 71–77.

KROHE, A. (1991): Emplacement of synkinematic plutons in the Variscan Odenwald (Germany) controlled by transtensional tectonics. – Geol. Rdsch., **80,** 391–409.

LAUE, S., REISCHMANN, T. & EMMERMANN, K. H. (1990): Geochemical variation of granitoid rocks from the NW margin of the Rhinegraben. – Beih. z. Europ. J. Mineral., **2/1,** 156.

LEEDER, M. R. (1982): Upper Paleozoic basins of the British Isles – Caledonide inheritance versus Hercynian plate margin processes. – J. geol. Soc. London, **139,** 479–491.

LIPPOLT, H. J. (1976): Nachweis altpaläozoischer Primäralter (Rb-Sr) und karbonischer Abkühlalter (K-Ar) der Muscovit-Biotit-Gneise des Spessarts und der Biotit-Gneise des Odenwaldes. – Geol. Rdsch., **75,** 569–583.

LORENZ, V. & NICHOLLS, I. A. (1984): Plate and intraplate processes of Hercynian Europe during the Late Paleozoic. – Tectonophysics, **107,** 25–56.

MASSONNE, H.-J. & SCHREYER, W. (1987): Phengite barometry based on the limiting assemblage with K-feldspar, phlogopite and quartz. – Contrib. Mineral. Petrol., **96,** 212–224.

MATTE, PH. (1986): Tectonics and Plate Tectonics Model for the Variscan Belt of Europe. – Tectonophysics, **126,** 329–374.

MEISL, St. (1990): Metavolcanic rocks in the 'Northern Phyllite Zone' at the southern margin of the Rhenohercynian belt. – Int. Conf. Paleozoic Orogens in Central Europe, Field Guide Mid German Crystalline Rise & Rheinisches Schiefergebirge, 25–42.

MONTIGNY, R., SCHNEIDER, C., ROYER, J. Y. & THUIZET, R. (1983): K-Ar dating of some plutonic rocks of the Vosges. – Terra Cognita, **3,** 201.

MÜNZING, K. (1956): Geologische Beobachtungen im Pfälzerwald. – Pfälzer Heimat, **7/1,** 14–16, Speyer.

NASIR, S., OKRUSCH, M., KREUZER, H., LENZ, H. & HÖHNDORF, A. (1991): Geochronology of the Spessart Crystalline Complex, Mid German Crystalline Rise. – Mineral. and Petrol., **44,** 39–55.

OKRUSCH, M. & RICHTER, P. (1986): Orthogneisses of the Spessart Crystalline Complex, Northwest Bavaria: Indicators of the geotectonic environment? Geol. Rdsch., **75,** 555–568.

—, VON RAUMER, J., MATTHES, S. & SCHUBERT, W. (1975): Mineralfazies und Stellung der Metamorphite im kristallinen Odenwald. – Aufschluß (Sonderband) 27 (Odenwald) 109–134.

ONCKEN, O. (1988): Aspects of the reconstruction of the stress history of a fold and thrust belt (Rhenish Massif, Federal Republic of Germany). – Tectonophysics, **152,** 19–40.

PLYUSNINA, L. P. (1982): Geothermometry and geobarometry of plagioclase – hornblende bearing assemblages. – Contrib. Mineral. Petrol., **80,** 140–146.

RAMSAY, J. R. (1980): The crack seal mechanism of rock deformation. – Nature, **248,** 135–139.

REITZ, E. (1987): Palynologie in metamorphen Serien: I. Silurische Sporen aus einem granatführenden Glimmerschiefer des Vor-Spessart. – N. Jb. Geol. Paläont. Mh., **1987,** 699–704.

SCHÄFER, A. (1989): Variscan molasse in the Saar-Nahe basin (W-Germany), Upper Carboniferous and Lower Permian. – Geol. Rdsch., **78,** 499–524.

SCHOLTZ, H. (1930): Das varistische Bewegungsbild. – Fortschr. Geol. u. Paläont. **VIII/25,** 235–316.

SOMMERMANN, A. (1990): Petrographie und Geochemie der magmatogenen Gerölle in Konglomeraten des Kulms im

Hinblick auf ihre Herkunft von der Mitteldeutschen Schwelle. – Geol. Jb. Hessen, **118,** 167–197.

SPEAR, F. S. (1980): NaSi – CaAl exchange equilibrium between plagioclase and amphibole. – An empirical model. – Contrib. Mineral. Petrol., **72,** 33–41.

– & CHENEY, J. T. (1989): A petrogenetic grid for pelitic schists in the system SiO_2-Al_2O_3-FeO-MgO-K_2O-H_2O. – Contrib. Mineral. Petrol., **101,** 149–164.

STELLRECHT, R. (1971): Geologisch-tektonische Entwicklung im Raum Albersweiler/Pfalz. Jber. u. Mitt. oberrh. geol. Ver., N.F., **53,** 239–262.

VOLL, G. (1976): Recrystallisation of quartz, biotite, and feldspars from Erstfeld to the Leventina Nappe, Swiss Alps, and its geological significance. – Schweiz. miner. petrogr. Mitt., **56,** 641–647.

WEBER, K. (1990): Crustal structure and the geological development of the Rhenohercynian/Saxothuringian terrane boundary in Central Europe. – Int. Conf. Paleozoic Orogens in Central Europe, Abstracts.

– & BEHR, H.-J. (1983): Geodynamic interpretation of the mid European Variscides. – In: Martin, H. & Eder, F. W. (eds.): Intracontinental Fold Belts, pp. 427–469, Heidelberg, New York, Tokyo, (Springer).

WICKERT, F. & EISBACHER, G. H. (1988): Two-sided Variscan thrust tectonics in the Vosges Mountains in northeastern France. – Geodin. Acta, **2/3,** 101–120.

—, ALTHERR, R. & DEUTSCH, M. (1990): Polyphase Variscan tectonics and metamorphism along a segment of the Saxothuringian-Moldanubian boundary: The Baden-Baden Zone, northern Schwarzwald (F.R.G.). – Geol. Rdsch., **79,** 627–647.

WILDBERG, H. G. H. (1990): Granitoide aus den saxothuringischen und moldanubischen Vogesen: Zeugen einer Entwicklung von Subduktion zu Kollision. – Beih. z. Europ. J. Mineral., **2/1,** 280.

WILLNER, A., MASSONNE, H. J. & KROHE, A. (1991): Tectonothermal evolution of a part of a Variscan magmatic arc: The Odenwald (FR Germany) as an example. – Geol. Rdsch., **80,** 369–390.

WONIK, T. & HAHN, A. (1989): Karte der Magnetfeldanomalien dF, Bundesrepublik Deutschland, Luxemburg, Schweiz und Österreich (westlicher Teil) 1:1.000.000. – Geol. Jb., **E43,** 3–21.

ZAMINER, C. (1957): Geologisch-petrographische Untersuchungen im Grundgebirge der Pfalz. – Mitt. Polichia III. Reihe, **4,** 7–33.

ZIEGLER, P. A. (1986): Geodynamic Model for the Paleozoic Crustal Consolidation of Western and Central Europe. – Tectonophysics, **126,** 303–328.